Modeling Earth Systems and Environment (2025)11:229
https://doi.org/10.1007/s40808-025-02394-z

ORIGINAL ARTICLE

A fractional derivative approach to infectious disease dynamics: modeling and optimal control strategies

Sayooj Aby Jose[1] · Raja Ramachandran[2] · Jirawattanapanit Anuwat[3] · Jinde Cao[4] · Ravi P. Agarwal[5]

Received: 22 December 2024 / Accepted: 17 March 2025

Abstract
This study presents a comprehensive analysis of infectious disease dynamics through mathematical modeling and optimal control strategies. The primary objective is to derive insights into disease transmission by employing a model structured on integer and Caputo fractional order derivatives (CFOD). Initially, we establish the feasible region and confirm the boundedness of the model. Subsequently, the disease-free equilibrium (DFE) points and the basic reproduction number ($\mathcal{R}_0$) are analytically determined. Using fixed point theory, we rigorously prove theoretical results relevant to the model. To approximate solutions, we apply the Modified Euler's Method (MEM), which demonstrates the model's capacity to simulate disease dynamics with increased realism. Finally, optimal control analysis reveals that an integrated application of all four control strategies significantly reduces the infected population, thus enhancing the recovery rate.

Keywords Caputo fractional order derivative · Equilibrium points · Infectious disease modeling · Modified Euler's Method · Optimal control strategies

Introduction

Humanity suffers from infectious diseases, which are both harmful and destructive. Sadly, millions of individuals die each year as a result of various sorts of those kind of diseases. The above point emphasises the necessity for more research on cognition and disease control. There are many unanswered concerns about how infectious diseases propagate. For instance, How much population will be completely impacted and hence need medication? How long will the population be affected by the epidemic? What can be done in the event of an infectious disease? Is it possible that the vaccination technique would minimise the occurrence and intensity of an epidemic? Infectious disease mathematical models are now used in public health decision-making. Modeling in epidemiology is extremely important since it may provide answers to the above concerns, as well as understand the fundamental process that regulates illness development and propose specific solutions for disease control. In order to understand and provide practical approaches for predicting and controlling the dynamics of infectious disease, mathematical modelling is critical (Hethcote 2000). Many researchers have built mathematical models to look at infectious disease transmission patterns and control mechanisms during the last few decades (Ahmed and El-Saka 2017; Chen and Li 2017; Lee et al. 2017; Kim et al. 2016; Thomas et al. 2022; Jose et al. 2022, 2023; Tahir et al. 2019; Wang and Chen 2022).

Infectious diseases are caused by harmful microorganisms such as bacteria, viruses, fungi, or parasites, which can travel directly or indirectly between people. Some of

✉ Raja Ramachandran
rajarchm2012@gmail.com

Sayooj Aby Jose
sayooaby999@gmail.com

Jirawattanapanit Anuwat
anuwat.j@pkru.ac.th

Jinde Cao
jdcao@seu.edu.cn

Ravi P. Agarwal
agarwalr@fit.edu

[1] Phuket Rajabhat University, Phuket, Thailand

[2] Alagappa University, Karaikudi, India

[3] Lebanese American University, Beirut, Lebanon

[4] Southeast University, Nanjing, China

[5] Florida Institute of Technology, Melbourne, USA

Published online: 24 April 2025

the most well-known infectious illnesses are influenza, TB, malaria, dengue fever, and more recent outbreaks such as COVID-19. Researchers have classified infectious illnesses over time based on how they are transferred-airborne, waterborne, vector-borne, or sexually transmitted. Each form of infection has its own transmission patterns, hence mathematical modeling is an important tool for understanding and limiting disease spread (Fantaye 2022; Fantaye et al. 2022; Khan et al. 2021; Nelson et al. 2024). Vaccination, quarantine, better sanitation, and medical interventions have all been used throughout history to slow the spread of infectious diseases. Modern epidemiology combines traditional approaches with data-driven computational models to improve forecast accuracy and public health responsiveness. This work expands on these fundamental epidemiological ideas by using fractional-order derivatives to increase disease transmission model accuracy.

Mathematical models that use an integer-order system of ODEs have been shown to be useful in understanding the structure of biological processes. Fractional-order models are chosen due to their ability to capture long-term dependencies and memory effects, which are crucial in infectious disease dynamics. Unlike classical integer-order models that assume instantaneous transitions, fractional derivatives allow for a more realistic representation of disease progression, incorporating the influence of past states on future dynamics. This approach provides deeper insights into the spread and control of infectious diseases and offers a more flexible and adaptable framework for modeling different epidemic scenarios (Teklu et al. 2024; Teklu 2024a; Fantaye and Birhanu 2023; Fantaye 2024). Panigoro et al. (2025) studied a two-predator, one-prey system with intra- and inter-specific competition using Caputo fractional derivatives, establishing stability conditions and identifying bifurcation behaviors. Herdicho et al. (2025) developed a COVID-19 model incorporating symptom severity, demonstrating improved accuracy over integer-order models and optimizing hospital resource allocation. Shamil et al. (2014) analyzed COVID-19 transmission in Thailand, integrating fractional derivatives to capture long-term memory effects and recommending mitigation strategies. Jose et al. (2024) introduced a fractional-order chickenpox model, validating its applicability through numerical simulations. These studies underscore the effectiveness of Caputo fractional derivatives in capturing complex dynamics across biological and ecological systems, improving predictive accuracy and informing decision-making. Fractional derivative operators on mathematical modeling are investigated by numerous publications and the dynamical behaviour of various pandemics have been extensively discussed under different circumstances (Khaminsou et al. 2021; Pinto and Carvalho 2017; Podlubny 1998; Zafar et al. 2017). Differential equations with a CFOD have been utilised to examine and analyse the transmission patterns of numerous infectious diseases (Carvalho et al. 2018; Sweilam et al. 2020; Tamilalagan et al. 2021). In Vargas-De-Léon (2015), the author explored uniform asymptotic stability of various primary epidemic models and the renowned Ross vector-borne diseases in Caputo sense using Volterra type Lyapunov functions.

In recent years, optimal control theory has been widely used in epidemiology to develop effective intervention techniques that reduce disease burden while making optimum use of existing resources. Optimal control is finding the most effective intervention measures-such as vaccination, quarantine, treatment, and awareness campaigns-for lowering infection rates and mitigating the effects of outbreaks (Teklu and Yohannes 2024; Teklu 2024b; Agusto and Khan 2018; Shen et al. 2021). This technique enables policymakers to assess different alternatives and select the most cost-effective and impactful solutions. Mathematically, optimum control issues are defined as minimizing an objective function (for example, the number of infected persons, economic expenses, or a mix of both). The model includes constraints such as limited medical resources and logistical practicality. The Pontryagin Maximum Principle (PMP) is often used to establish required conditions for optimality, allowing researchers to identify how treatments should be deployed over time to get the greatest potential outcomes.

Unexpected infectious illness outbreaks have a variety of economic consequences on a worldwide scale. The first noticeable impact, for example, could be preventative and restraint actions adopted by governments with few resources. Optimal control theory is defined as a branch of mathematical optimization interested in controlling a dynamical system in order to minimise or maximise an objective function over time. Optimal control strategies act as a crucial role during the invasion phase for the powerful use of few resources. In mathematical models of Ebola, Zika, HIV, and TB, the theory of optimal control has been utilized often (Area et al. 2018; Silva et al. 2017; Silva and Torres 2018). The view of infectious models is linked to the view of control methods like education campaigns (Castilho 2006), resource allocation (Ball and Becker 2006), and vaccination (Brandeau et al. 2003).

The purpose of this study is to propose and study a more accurate mathematical model of the transmission of infectious diseases based on integer and CFOD. We investigated the optimal control problem associated with our given model. We numerically investigated the dynamical system in relation to parameter values associated with the model. The final portion includes some interesting observations based on our numerical analysis.

This paper's remaining sections are arranged as follows: The mathematical model that describes the dynamics of infectious disease transmission is formulated in Sect. 2 and includes both integer-order and Caputo fractional-order variants. In order to identify the critical parameters affecting the spread of illness, we examine the model's basic characteristics in Sect. 3, including equilibrium points, stability analysis using the Routh–Hurwitz criterion, and sensitivity analysis. In order to improve the accuracy of epidemic forecasts and provide a more realistic depiction of disease dynamics, Sect. 4 presents the fractional-order version of the model utilizing Caputo derivatives. Using the Pontryagin Maximum Principle, we create an ideal control plan in Sect. 5 to reduce infection rates through hospitalization, treatment, and prevention. Numerical simulations employing the Modified Euler's Method are presented in Sect. 6 to support theoretical conclusions and show how fractional-order derivatives affect the course of illness. The main findings are finally outlined in Section 7, which also makes recommendations for future study approaches, such as incorporating stochastic effects and validating data from real-world scenarios.

Model framework: integer order model

The model addressed in this paper is a modification to the transmission dynamics of infectious disease model. The susceptible, exposed, symptomatic infected, asymptomatic infected, hospitalised, and recovered populations are considered in a $T_S T_E T_I T_A T_H T_R$ compartmental model. The model's transmission flow is depicted in the diagram below (Fig. 1).

This model is not disease-specific; rather, it reflects a basic framework for infectious diseases. Acute infectious diseases with an exposed (latent) period prior to symptom onset are a good fit for the framework. However, adjustments to the model structure and parameter values would be necessary for realistic depiction of illnesses with distinct transmission methods or long-term progression features.

Based on the nature of the disease and the immune system's reaction, people may either develop symptoms (T_I) or stay asymptomatic (T_A) following the exposure period (T_E). While asymptomatic people may still aid in the spread of disease, symptomatic people show clinical indicators. This study assumes a fixed categorization post-exposure, meaning that once individuals are classified, they stay in their respective groups until they recover. However, if needed, transitions between these groups might be included in future additions.

We formulate the following model,

$$\begin{aligned}
\frac{dT_S(t)}{dt} &= A - \pi T_S(t)\big(T_I(t) + \kappa T_A(t)\big) + \nu T_E(t) - \vartheta T_S(t)\\
\frac{dT_E(t)}{dt} &= \pi T_S(t)\big(T_I(t) + \kappa T_A(t)\big) - (\sigma + \nu + \vartheta)T_E(t)\\
\frac{dT_I(t)}{dt} &= \eta\sigma T_E(t) - (\psi_1 + \vartheta + \vartheta_1 + \xi_1)T_I(t)\\
\frac{dT_A(t)}{dt} &= (1-\eta)\sigma T_E(t) - (\psi_2 + \vartheta + \vartheta_2 + \xi_2)T_A(t)\\
\frac{dT_H(t)}{dt} &= \xi_1 T_I(t) + \xi_2 T_A(t) - (\psi_3 + \vartheta)T_H(t)\\
\frac{dT_R(t)}{dt} &= \psi_1 T_I(t) + \psi_2 T_A(t) + \psi_3 T_H(t) - \vartheta T_R(t)
\end{aligned} \tag{1}$$

The initial conditions of the system are,

$$T_S(0) = T_{S_0}, T_E(0) = T_{E_0}, T_I(0) = T_{I_0}, T_A(0) = T_{A_0}, T_H(0) = T_{H_0}, T_R(0) = T_{R_0}.$$

Here, N is total population, divided into $T_S(t), T_E(t), T_I(t), T_A(t), T_H(t)$ and $T_R(t)$ at time t. The recruitment rate is denoted by A. Let $\pi = \pi_1 + \pi_2$, where π_1 is the rate of virus transmission from direct contact from living organism and π_2 is the rate of virus transmission from indirect contact or nonliving organism. Contact rates from the asymptomatic to the susceptible population is denoted by κ. An exposed individual's incubation period is

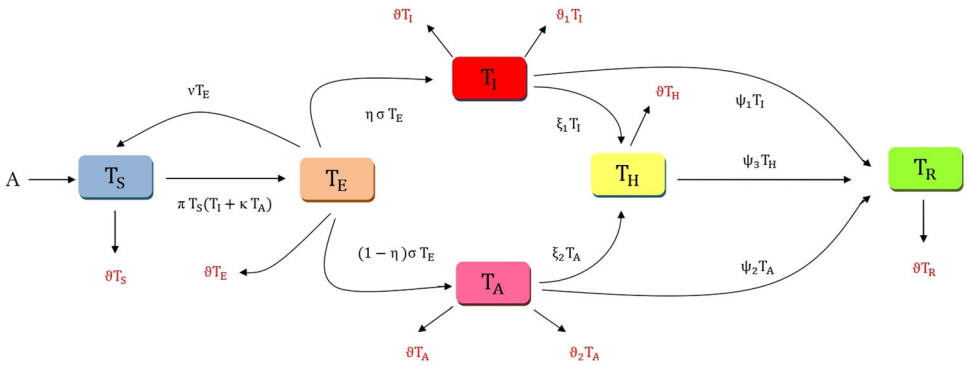

Fig. 1 Schematic diagram for the transmission dynamics of infectious disease

denoted by σ, and the proportion of the population exposed which becomes symptomatic afterwards the incubation period is denoted by η leaving $(1-\eta)$ population asymptomatic. The precaution and natural immunity is denoted by ν. ψ_1, ψ_2 and ψ_3 denotes the recovery date of symptomatic, asymptomatic and hospitalized individuals respectively. ξ_1 is the proportion of being hospitalized from symptomatic and ξ_2 is the proportion of being hospitalized from asymptomatic. Natural death rate is ϑ whereas ϑ_1 and ϑ_2 are mortality rates of the symptomatic, and asymptomatic populations respectively. Table 1 provides a summary of the parameters and variables used in the model, along with their descriptions and units.

Existence and uniqueness of solution

Theorem 2.1 *Consider $\ell \in \mathbb{R}^+$. The dynamical system (1) admits a unique solution on interval $(0,\ell)$ for initial conditions satisfying* $T_S(0)>0, T_E(0)>0, T_I(0)>0, T_A(0)>0, T_H(0)>0, T_R(0)>0$.

Proof Let, $\theta(t)=(T_S,T_E,T_I,T_A,,T_H,T_R)^T$, then (1) become $\frac{d\theta}{dt}=\mathcal{U}(\theta(t))=(u_1,u_2,u_3,u_4,\ u_5,u_6)^T$. Suppose the initial condition $\theta(0)=(T_S(0),T_E(0),T_I(0),T_A(0),T_H(0),T_R(0))^T>0$. When the Jacobian $\mathcal{J}\big(\mathcal{U}(\theta(t))\big)$ is computed and examined, the RHS of (1), namely $\mathcal{U}$ and its Jacobian, is continuous for $t>0$. As a result, on $\mathbb{R}^6_+$, $\mathcal{U}$ satisfies a Lipschitz condition. Picard-Lindelof theorem proves the existence and uniqueness of a solution for a certain time interval $(0,\ell)$. □

Theorem 2.2 (*Positivity of solution*) *With non-negative initial data, the state variables T_S,T_E,T_I,T_A,T_H,T_R of (1) remain non-negative for every $t>0$.*

Proof Let $T_S(0)=T_{S_0}>0$. From the first equation of (1),

$$\frac{dT_S}{dt}\geq -\Big(\pi\big(T_I(t)+\kappa T_A(t)\big)+\vartheta\Big)T_S(t)$$

and integration, $T_S(t)\geq T_{S_0}e^{-(\vartheta t+b)}>0$ for all $t>0, b=\int_0^t\big(T_I(\varrho)-\kappa T_A(\varrho)\big)d\varrho$.

Similarly we get

$$T_E(t)\geq T_{E_0}e^{-(\sigma+\nu+\vartheta)t}>0$$
$$T_I(t)\geq T_{I_0}e^{-(\psi_1+\vartheta+\vartheta_1+\xi_1)t}>0$$
$$T_A(t)\geq T_{A_0}e^{-(\psi_2+\vartheta+\vartheta_2+\xi_2)t}>0$$
$$T_H(t)\geq T_{H_0}e^{-(\psi_3+\vartheta)t}>0$$
$$T_R(t)\geq T_{R_0}e^{-(\vartheta)t}>0$$

therefore, proved non-negativity of the remaining state variables. □

Boundedness of solution

Theorem 2.3 *The integer order model (1) has solutions bounded within invariant region given by* $\Delta=\Big\{(T_S,T_E,T_I,T_A,T_H,T_R)\in\mathbb{R}^6_+\mid 0\leq T_S, T_E,T_I,T_A,T_H,T_R\leq\frac{A}{\vartheta}\Big\}$.

Proof We have $N(t)=T_S+T_E+T_I+T_A+T_H+T_R$. Then $\frac{dN}{dt}\leq A-\vartheta N(t)$. Consider the initial valued problem

Table 1 Model variables and parameters

Symbol	Description	Unit
A	Recruitment rate of susceptible individuals	per day
π	Disease transmission rate	per day
ϑ	Natural death rate	per day
σ	Disease progression rate of infectious of exposed individuals	per day
η	Proportion of infectious individuals that are showing symptoms	per day
ψ_1	Recovery rate of symptomatic individuals recovering	per day
ψ_2	Recovery rate of asymptomatic individuals recovering	per day
ψ_3	Recovery rate of hospitalized individuals recovering	per day
ξ_1	Hospitalization rate of symptomatic individuals	per day
ξ_2	Hospitalization rate of asymptomatic individuals	per day
ν	Precaution and natural immunity rate	per day
κ	Contact rates from the asymptomatic to the susceptible population	per day
ϑ_1	Death rate of symptomatic individuals	per day
ϑ_2	Death rate of asymptomatic individuals	per day

$N^{'}(t) \leq A - \vartheta N(t), N(0) = N_0$ and comparison theorem (McNabb 1986),

$$N(t) \leq N_0 e^{-\vartheta t} + \frac{A}{\vartheta}(1 - e^{-\vartheta t})$$

and consequently $\limsup_{t\to\infty} N(t) \leq \frac{A}{\vartheta}$. □

Local stability

The newly infected persons that emerges from any sick persons in a totally susceptible population is expected to be specified by $\mathcal{R}_0$, the basic reproduction number. $\mathcal{R}_0$ is also not a rate, as it is a dimensionless quantity with units of time^{-1}. The Disease Free Equilibrium (DFE) of an epidemic system is locally asymptotically stable if $\mathcal{R}_0 < 1$ holds (If the initial circumstances of the variables T_S, T_E, T_I, T_A, T_H and T_R are surroundings of the DFE, the disease is eradicated from the individuals). If there is an outbreak in the community, the discovery of situations that may provide $\mathcal{R}_0 < 1$ has significant public health implications. System (1) admits a single DFE point $\mathscr{D}^\circ = (T_S^\circ, T_E^\circ, T_I^\circ, T_A^\circ, T_H^\circ, T_R^\circ) = (\frac{A}{\vartheta}, 0, 0, 0, 0, 0)$ in the absence of disease. To establish the existence and uniqueness of an Endemic Equilibrium (EE) $\mathscr{D}^\star = (T_S^\star, T_E^\star, T_I^\star, T_A^\star, T_H^\star, T_R^\star)$, we first compute the system's fundamental reproductive number $\mathcal{R}_0$ of system (1) using the Next-Matrix generation approach (Driessche and Watmough 2002).

$$\mathcal{F} = \begin{pmatrix} \pi T_S(t)\big(T_I(t) + \kappa T_A(t)\big) \\ 0 \\ 0 \end{pmatrix} \text{and} \mathcal{N} = \begin{pmatrix} (\sigma + \nu + \vartheta)T_E(t) \\ (\psi_1 + \vartheta + \vartheta_1 + \xi_1)T_I(t) - \eta\sigma T_E(t) \\ (\psi_2 + \vartheta + \vartheta_2 + \xi_2)T_A(t) - (1-\eta)\sigma T_E(t) \end{pmatrix}$$

Here we get

$$\Im = \begin{pmatrix} 0 & \frac{A\pi}{\vartheta} & \frac{A\eta\pi}{\vartheta} \\ 0 & 0 & 0 \\ 0 & 0 & 0 \end{pmatrix} \text{and}$$

$$\aleph = \begin{pmatrix} (\sigma + \nu + \vartheta) & 0 & 0 \\ -\eta\sigma & (\psi_1 + \vartheta + \vartheta_1 + \xi_1) & 0 \\ -(1-\eta)\sigma & 0 & (\psi_2 + \vartheta + \vartheta_2 + \xi_2) \end{pmatrix}$$

Now, using T_E, T_I and T_A from system (1), compute the fundamental reproductive ratio $\mathcal{R}_0$ using the next-generation matrix approach. The next-generation matrix is made up of the matrices $\Im$ and $\aleph^{-1}$, where the matrix $\Im$ represents the rate of transmission of infection in these categories and the matrix $\aleph$ describes all other transmissions between them. $\mathcal{R}_0$ is obtained as follows,

$$\mathcal{R}_0 = \rho(\Im\aleph^{-1}) = \frac{A\pi\sigma\Big[\eta(\psi_2 + \vartheta + \vartheta_2 + \xi_2) + (1-\eta)\kappa(\psi_1 + \vartheta + \vartheta_1 + \xi_1)\Big]}{\vartheta(\sigma + \nu + \vartheta)(\psi_1 + \vartheta + \vartheta_1 + \xi_1)(\psi_2 + \vartheta + \vartheta_2 + \xi_2)} = \mathcal{R}_{01} + \mathcal{R}_{02}$$

where,

$$\mathcal{R}_{01} = \frac{A\pi\sigma\eta}{\vartheta(\sigma + \nu + \vartheta)(\psi_1 + \vartheta + \vartheta_1 + \xi_1)},$$

$$\mathcal{R}_{02} = \frac{A\pi\sigma(1-\eta)\kappa}{\vartheta(\sigma + \nu + \vartheta)(\psi_2 + \vartheta + \vartheta_2 + \xi_2)}.$$

system (1) admits $\mathscr{D}^\star = (T_S^\star, T_E^\star, T_I^\star, T_A^\star, T_H^\star, T_R^\star)$ as a unique endemic equilibrium point, where

$$T_S^\star = \frac{A}{\vartheta\mathcal{R}_0}$$

$$T_E^\star = A\left(1 - \frac{1}{\mathcal{R}_0}\right)\mathcal{N}$$

$$T_I^\star = \frac{\eta\sigma}{(\psi_1 + \vartheta + \vartheta_1 + \xi_1)}T_E^\star$$

$$T_A^\star = \frac{(1-\eta)\sigma}{(\psi_2 + \vartheta + \vartheta_2 + \xi_2)}T_E^\star$$

$$T_H^\star = \frac{\mathcal{N}_1}{\mathcal{N}_2}T_E^\star$$

$$T_R^\star = \frac{\mathcal{N}_2\big(\eta\sigma\psi_1(\psi_2 + \vartheta + \vartheta_2 + \xi_2) + \psi_2(1-\eta)\sigma(\psi_1 + \vartheta + \vartheta_1 + \xi_1)\big) + \mathcal{N}_1\big(\vartheta(\psi_1 + \vartheta + \vartheta_1 + \xi_1)(\psi_2 + \vartheta + \vartheta_2 + \xi_2)\big)}{\mathcal{N}_2\vartheta(\psi_1 + \vartheta + \vartheta_1 + \xi_1)(\psi_2 + \vartheta + \vartheta_2 + \xi_2)}T_E^\star$$

where,

$$\mathcal{N} = \left(\frac{1}{(\sigma+\nu+\vartheta+\nu)}\right)$$
$$\mathcal{N}_1 = \xi_1\eta\sigma(\psi_2+\vartheta+\vartheta_2+\xi_2)+\xi_2(1-\eta)\sigma(\psi_1+\vartheta+\vartheta_1+\xi_1)$$
$$\mathcal{N}_2 = (\psi_3+\vartheta)(\psi_1+\vartheta+\vartheta_1+\xi_1)(\psi_2+\vartheta+\vartheta_2+\xi_2)$$

Clearly, it is evident that if $\mathcal{R}_0<1$, then (1) doesn't take any positive endemic equilibrium. Thus, we require $\mathcal{R}_0>1$, to ensure the existence and positivity of the endemic equilibrium point.

Theorem 2.4 *If $\mathcal{R}_0<1$, then the disease-free equilibrium $\mathscr{D}^\circ$ of system (1) is asymptotically stable on Δ.*

Proof The Jacobian matrix of system (1) is given by,

$$\mathcal{J} = \begin{pmatrix} -\pi\left(T_I+\kappa T_A\right)-\vartheta & \nu & -\pi T_S & -\pi\kappa T_S & 0 & 0 \\ \pi\left(T_I+\kappa T_A\right) & -(\sigma+\nu+\vartheta) & \pi T_S & \pi\kappa T_S & 0 & 0 \\ 0 & \eta\sigma & -(\psi_1+\vartheta+\vartheta_1+\xi_1) & 0 & 0 & 0 \\ 0 & (1-\eta)\sigma & 0 & -(\psi_2+\vartheta+\vartheta_2+\xi_2) & 0 & 0 \\ 0 & 0 & \xi_1 & \xi_2 & -(\psi_3+\vartheta) & 0 \\ 0 & 0 & \psi_1 & \psi_2 & \psi_3 & -\vartheta \end{pmatrix} \tag{2}$$

Then we figure out the Jacobian matrix at $\mathscr{D}^\circ$ as,

$$\mathcal{J}_{\mathscr{D}^\circ} = \begin{pmatrix} -\vartheta & \nu & \frac{-\pi A}{\vartheta} & \frac{-\pi\kappa A}{\vartheta} & 0 & 0 \\ 0 & -(\sigma+\nu+\vartheta) & \frac{\pi A}{\vartheta} & \frac{\pi\kappa A}{\vartheta} & 0 & 0 \\ 0 & \eta\sigma & -(\psi_1+\vartheta+\vartheta_1) & 0 & 0 & 0 \\ 0 & (1-\eta)\sigma & 0 & -(\psi_2+\vartheta+\vartheta_2) & 0 & 0 \\ 0 & 0 & \xi_1 & \xi_2 & -(\psi_3+\vartheta) & 0 \\ 0 & 0 & \psi_1 & \psi_2 & \psi_3 & -\vartheta \end{pmatrix}$$

It can be seen that the matrix $\mathcal{J}_{\mathscr{D}_1}$ has the eigenvalues, $-\vartheta, -(\psi_3+\vartheta), -\vartheta$. The rest of the four eigenvalues of the Jacobian matrix $\mathcal{J}_{\mathscr{D}_1}$ can computed from the following equation:

$$\lambda^3+\mathscr{L}_1\lambda^2+\mathscr{L}_2\lambda+\mathscr{L}_3=0$$
$$\mathscr{L}_1=(l_1+l_2+l_3),\mathscr{L}_2=((1-\mathcal{R}_{01})l_1l_2+(1-\mathcal{R}_{02})l_1l_3+l_2l_3),$$
$$\mathscr{L}_3=(1-\mathcal{R}_0)l_1l_2l_3$$
$$l_1=(\sigma+\nu+\vartheta),l_2=(\psi_1+\vartheta+\vartheta_1+\xi_1),l_3=(\psi_2+\vartheta+\vartheta_2+\xi_2)$$

Now, $\mathscr{L}_1\mathscr{L}_2-\mathscr{L}_3=(l_1+l_2+l_3)\left[(1-\mathcal{R}_{01})l_1l_2+(1-\mathcal{R}_{02})l_1l_3\right]+l_2^2l_3+l_2l_3^2+\mathcal{R}_0l_1l_2l_3>0$

Since all $l_i>0$, where $i=1,2,3$, from the above we can easily seen that $\mathscr{L}_i>0$, where $i=1,2,3$, only if $\mathcal{R}_1<1$. Hence by Routh Hurwitz's theorem we can says that the $\mathscr{D}_1$ is locally asymptotically stable if $\mathcal{R}_1<1$. □

Theorem 2.5 *Assume that $\mathcal{R}_0>1$; then, the unique $\mathscr{D}^\star$ of system (1) is asymptotically stable on Δ.*

Proof The Jacobian matrix of (1) at $\mathscr{D}^\star$ defined as,

$$\mathcal{J}_{\mathscr{D}^\star} = \begin{pmatrix} -\mathcal{G}-\vartheta & \nu & \frac{-\pi A}{\vartheta\mathcal{R}_0} & \frac{-\pi\kappa A}{\vartheta\mathcal{R}_0} & 0 & 0 \\ \mathcal{G} & -(\sigma+\nu+\vartheta) & \frac{\pi A}{\vartheta\mathcal{R}_0} & \frac{\pi\kappa A}{\vartheta\mathcal{R}_0} & 0 & 0 \\ 0 & \eta\sigma & -(\psi_1+\vartheta+\vartheta_1+\xi_1) & 0 & 0 & 0 \\ 0 & (1-\eta)\sigma & 0 & -(\psi_2+\vartheta+\vartheta_2+\xi_2) & 0 & 0 \\ 0 & 0 & \xi_1 & \xi_2 & -(\psi_3+\vartheta) & 0 \\ 0 & 0 & \psi_1 & \psi_2 & \psi_3 & -\vartheta \end{pmatrix}$$

where $\mathcal{G} = (\mathcal{R}_0 - 1)\mathcal{N}\vartheta(\sigma+\nu+\vartheta)$ It can be seen that the matrix $\mathcal{J}_{\mathscr{D}_\star}$ has the eigenvalue, $-\vartheta$ The rest of the four eigenvalues of the Jacobian matrix $\mathcal{J}_{\mathscr{D}^\star}$ can computed from the following equation:

$$\begin{aligned}
&\lambda^4+\mathscr{L}_1\lambda^3+\mathscr{L}_2\lambda^2+\mathscr{L}_3\lambda+\mathscr{L}_4=0\\
&\mathscr{L}_1=(\mathcal{G}+\vartheta+l_1+l_2+l_3),\mathscr{L}_2=((\mathcal{G}+\vartheta)(l_1+l_2+l_3)\\
&+(1-\frac{\mathcal{R}_{01}}{\mathcal{R}_0})l_1l_2+(1-\frac{\mathcal{R}_{02}}{\mathcal{R}_0})l_1l_3+l_2l_3+\nu\mathcal{G}),\\
&\mathscr{L}_3=(\mathcal{G}+\vartheta)\left(l_1l_2+l_1l_3+l_2l_3\right)\\
&+l_2\left(\nu\mathcal{G}-\frac{l_1\mathcal{R}_{01}}{\mathcal{R}_0}\right)+l_3\left(\nu\mathcal{G}-\frac{l_1\mathcal{R}_{02}}{\mathcal{R}_0}\right),\mathscr{L}_4=\mathcal{G}l_2l_3(\nu+l_1)\\
&l_1=(\sigma+\nu+\vartheta),l_2=(\psi_1+\vartheta+\vartheta_1),l_3=(\psi_2+\vartheta+\vartheta_2)
\end{aligned}$$

Now, $\mathscr{L}_1\mathscr{L}_2-\mathscr{L}_3>0, \mathscr{L}_1(\mathscr{L}_2\mathscr{L}_3-\mathscr{L}_1\mathscr{L}_4)>0$

Since all $l_i>0$, where $i=1,2,3$, from the above we can easily seen that $\mathscr{L}_i>0$, where $i=1,2,3,4$, only if $\mathcal{R}_1>1$. Hence by Routh Hurwitz's theorem we can says that the the unique endemic equilibrium $\mathscr{D}^\star$ of system (1) is asymptotically stable on Δ. □

Theorem 2.6 *If $\mathcal{R}_0<1$, then the disease-free equilibrium $\mathscr{D}^\circ$ of system (1) is globally asymptotically stable on Δ.*

Proof The Lyapunov function is defined as:

$$V(T_E,T_I,T_A)=c_1T_E+c_2T_I+c_3T_A.$$

Taking the time derivative:

$$\frac{dV}{dt}=c_1\frac{dT_E}{dt}+c_2\frac{dT_I}{dt}+c_3\frac{dT_A}{dt}.$$

Substituting the system equations:

$$\begin{aligned}
\frac{dT_E}{dt}&=\pi T_S(T_I+\kappa T_A)-(\sigma+\nu+\vartheta)T_E,\\
\frac{dT_I}{dt}&=\eta\sigma T_E-(\psi_1+\vartheta+\vartheta_1+\xi_1)T_I,\\
\frac{dT}{dt}&=(1-\eta)\sigma T_E-(\psi_2+\vartheta+\vartheta_2+\xi_2)T_A.
\end{aligned}$$

At the disease-free equilibrium, $T_S=\frac{A}{\vartheta}$, so:

$$\begin{aligned}
\frac{dV}{dt}=&c_1\left(\frac{A}{\vartheta}\pi(T_I+\kappa T_A)-(\sigma+\nu+\vartheta)T_E\right)\\
&+c_2(\eta\sigma T_E-(\psi_1+\vartheta+\vartheta_1+\xi_1)T_I)\\
&+c_3((1-\eta)\sigma T_E-(\psi_2+\vartheta+\vartheta_2+\xi_2)T_A)
\end{aligned}$$

To cancel terms, we set:

$$\begin{aligned}
c_2&=\frac{c_1\pi A}{\vartheta(\psi_1+\vartheta+\vartheta_1+\xi_1)}\\
c_3&=\frac{c_1\pi A\kappa}{\vartheta(\psi_2+\vartheta+\vartheta_2+\xi_2)}.
\end{aligned}$$

Substituting these into $\frac{dV}{dt}$:

$$\begin{aligned}
\frac{dV}{dt}&=-c_1(\sigma+\nu+\vartheta)T_E\\
&+\frac{c_1\pi A}{\vartheta}T_E\left(\frac{\eta\sigma}{\psi_1+\vartheta+\vartheta_1+\xi_1}+\kappa\frac{(1-\eta)\sigma}{\psi_2+\vartheta+\vartheta_2+\xi_2}\right)
\end{aligned}$$

From the definition:

$$\begin{aligned}
\mathcal{R}_0=&\frac{A\pi\sigma}{\vartheta(\sigma+\nu+\vartheta)(\psi_1+\vartheta+\vartheta_1+\xi_1)(\psi_2+\vartheta+\vartheta_2+\xi_2)}\\
&\times[\eta(\psi_2+\vartheta+\vartheta_2+\xi_2)+(1-\eta)\kappa(\psi_1+\vartheta+\vartheta_1+\xi_1)].
\end{aligned}$$

Rewriting the term in brackets:

$$\frac{\pi A}{\vartheta}\left(\frac{\eta\sigma}{\psi_1+\vartheta+\vartheta_1+\xi_1}+\kappa\frac{(1-\eta)\sigma}{\psi_2+\vartheta+\vartheta_2+\xi_2}\right)=(\sigma+\nu+\vartheta)R_0.$$

Thus,

$$\frac{dV}{dt}=c_1T_E(\sigma+\nu+\vartheta)(R_0-1).$$

If $\mathcal{R}_0<1$, then $\frac{dV}{dt}\le 0$. The only time $\frac{dV}{dt}=0$ is when $T_E=0$, implying $T_I=0, T_A=0$. Applying LaSalle's Invariance Principle, the system converges to the disease-free equilibrium (DFE). Thus, proving global stability when $\mathcal{R}_0<1$. □

Sensitivity analysis

This section employs the theory of sensitivity analysis to establish the importance of the generic parameters identified in $\mathcal{R}_0$. Furthermore, parameter values derived from

valid assumptions are used to generate both numerical and analytic values of $\mathcal{R}_0$. The dynamics follow the model if and only if the generated analytic expressions can be utilized to give insight on how to regulate the model's start in various locations. Here $\mathcal{R}_0$ is the threshold value since reducing it below unity is regarded to be the most effective way of controlling and stopping disease spread. The sensitivity index technique identifies the most sensitive parameters of the model. Those with a positive sign are highl sensitive to increasing $\mathcal{R}_0$, while those with a negative sign are less sensitive to decreasing $\mathcal{R}_0$, and the remaining is neutrally sensitive (with zero relative sensitivity). For more information, see Chitnis et al. (2008). This analysis deals with the investigation of $\mathcal{R}_0$ sensitivity to each parameters.

$$\wedge_{\flat}^{\mathcal{R}_0} = \frac{\partial \mathcal{R}_0}{\partial \flat} \times \frac{\flat}{\mathcal{R}_0}$$

for $\flat$ represents all the basic parameters and

Table 2 Numerical sensitivity index values for ($\mathcal{R}_0$)

Parameter	Sensitivity index value
S_A	1.0000
S_π	1.0000
S_η	0.2528
S_{ψ_1}	−0.2249
S_{ψ_2}	−0.2632
S_{ϑ_1}	−0.0026
S_{ϑ_2}	0.0239
S_{ξ_1}	−0.0312
S_{ξ_2}	−0.4539
S_ν	−0.9994
S_σ	0.9995
S_ϑ	− 1

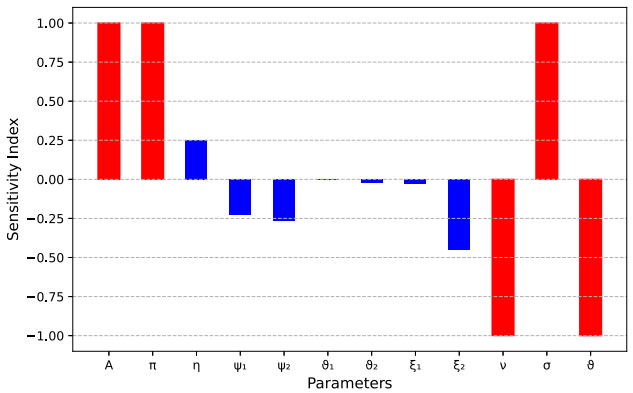

Fig. 2 Sensitivity index diagram

$$R_0 = \frac{A\pi\sigma\left[\eta(\psi_2+\vartheta+\vartheta_2+\xi_2)+(1-\eta)\kappa(\psi_1+\vartheta+\vartheta_1+\xi_1)\right]}{\vartheta(\sigma+\nu+\vartheta)(\psi_1+\vartheta+\vartheta_1+\xi_1)(\psi_2+\vartheta+\vartheta_2+\xi_2)}$$

then

$$\wedge_A^{\mathcal{R}_0} = 1$$

$$\wedge_\pi^{\mathcal{R}_0} = 1$$

$$\wedge_\eta^{\mathcal{R}_0} = \frac{1}{1+\dfrac{\kappa(\psi_1+\vartheta+\vartheta_1+\xi_1)}{\eta(\psi_2+\vartheta+\vartheta_2+\xi_2-\kappa(\psi_1+\vartheta+\vartheta_1+\xi_1)}}$$

$$\wedge_{\psi_1}^{\mathcal{R}_0} = \frac{-\eta\psi_1(\psi_2+\vartheta+\vartheta_2+\xi_2)}{(\psi_1+\vartheta+\vartheta_1+\xi_1)\left[\eta(\psi_2+\vartheta+\vartheta_2+\xi_2)+(1-\eta)\kappa(\psi_1+\vartheta+\vartheta_1+\xi_1)\right]}$$

$$\wedge_{\psi_2}^{\mathcal{R}_0} = \frac{-(1-\eta)\kappa\psi_2(\psi_1+\vartheta+\vartheta_1+\xi_1)}{(\psi_2+\vartheta+\vartheta_2+\xi_2)\left[\eta(\psi_2+\vartheta+\vartheta_2+\xi_2)+(1-\eta)\kappa(\psi_1+\vartheta+\vartheta_1+\xi_1)\right]}$$

$$\wedge_{\vartheta_1}^{\mathcal{R}_0} = \frac{-\eta\vartheta_1(\psi_2+\vartheta+\vartheta_2+\xi_2)}{(\psi_1+\vartheta+\vartheta_1+\xi_1)\left[\eta(\psi_2+\vartheta+\vartheta_2+\xi_2)+(1-\eta)\kappa(\psi_1+\vartheta+\vartheta_1+\xi_1)\right]}$$

$$\wedge_{\vartheta_2}^{\mathcal{R}_0} = \frac{(1-\eta)\kappa\vartheta_2(\psi_1+\vartheta+\vartheta_1+\xi_1)}{(\psi_2+\vartheta+\vartheta_2+\xi_2)\left[\eta(\psi_2+\vartheta+\vartheta_2+\xi_2)+(1-\eta)\kappa(\psi_1+\vartheta+\vartheta_1+\xi_1)\right]}$$

$$\wedge_{\xi_1}^{\mathcal{R}_0} = \frac{-\eta\xi_1(\psi_2+\vartheta+\vartheta_2+\xi_2)}{(\psi_1+\vartheta+\vartheta_1+\xi_1)\left[\eta(\psi_2+\vartheta+\vartheta_2+\xi_2)+(1-\eta)\kappa(\psi_1+\vartheta+\vartheta_1+\xi_1)\right]}$$

$$\wedge_{\xi_2}^{\mathcal{R}_0} = \frac{(1-\eta)\kappa\xi_2(\psi_1+\vartheta+\vartheta_1+\xi_1)}{(\psi_2+\vartheta+\vartheta_2+\xi_2)\left[\eta(\psi_2+\vartheta+\vartheta_2+\xi_2)+(1-\eta)\kappa(\psi_1+\vartheta+\vartheta_1+\xi_1)\right]}$$

$$\wedge_\nu^{\mathcal{R}_0} = \frac{-\nu}{(\sigma+\nu+\vartheta)}$$

$$\wedge_\sigma^{\mathcal{R}_0} = \frac{\nu+\vartheta}{(\sigma+\nu+\vartheta)}$$

$$\wedge_\vartheta^{\mathcal{R}_0} = \vartheta\left(\frac{(\eta+(1-\eta)\kappa)}{\eta(\psi_2+\vartheta+\vartheta_2+\xi_2)+(1-\eta)\kappa(\psi_1+\vartheta+\vartheta_1+\xi_1)} - \frac{B}{\widehat{B}}\right)$$

where

$$\begin{aligned} B =& (\sigma+\nu+\vartheta)(\psi_1+\vartheta+\vartheta_1+\xi_1)(\psi_2 \\ &+\vartheta+\vartheta_2+\xi_2)+\vartheta(\psi_1+\vartheta+\vartheta_1+\xi_1)(\psi_2+\vartheta+\vartheta_2+\xi_2) \\ &+\vartheta(\sigma+\nu+\vartheta)(\psi_2+\vartheta+\vartheta_2+\xi_2) \\ &+\vartheta(\sigma+\nu+\vartheta)(\psi_1+\vartheta+\vartheta_1+\xi_1) \end{aligned}$$

$$\widehat{B} = \vartheta(\sigma+\nu+\vartheta)(\psi_1+\vartheta+\vartheta_1+\xi_1)(\psi_2+\vartheta+\vartheta_2+\xi_2)$$

We can observe that some of the parameters have positive relationships and some others have negative relationships. A negative relationship indicates that increasing the value of this parameter helps to diminish the severity of the infection. A positive connection indicates that increasing the value of that parameters will have a significant impact

on the frequency with which the ailment spreads. The sensitivity indices are presented in Table 2, and the corresponding plots are shown in Fig. 2.

From the computed sensitivity indices, we observe that some parameters have a positive relationship with $\mathcal{R}_0$, while others have a negative relationship.

Positive Sensitivity Indices: Parameters such as A, π, σ η and increase the basic reproduction number $\mathcal{R}_0$, meaning that higher values of these parameters lead to a greater spread of the disease. This suggests that controlling infection transmission π and reducing the exposed-to-infected progression rate σ are critical in disease mitigation.

Negative Sensitivity Indices: Parameters like ξ_1, ξ_2, v, ϑ, and ζ_2 negatively affect $\mathcal{R}_0$, meaning that increasing these values reduces the severity of the infection. For instance, higher recovery rates (ξ_1, ξ_2), help lower disease prevalence, while natural immunity v and natural death rate ϑ also play roles in reducing transmission.

The most influential parameters in disease control are those with sensitivity indices close to 1 or – 1, such as π, σ, v and ϑ. This means interventions targeting these parameters will be the most effective in reducing disease spread.

The sensitivity plots Fig. 2 visually represent the impact of each parameter on R_0 Bars above zero (positive indices) indicate parameters that increase $\mathcal{R}_0$ when their values rise. Bars below zero (negative indices) represent parameters that help reduce R_0 when increased. This highlights that effective intervention strategies should focus on reducing transmission rate π and progression rate σ, while enhancing recovery rates (ξ_1, ξ_2), and immunity v.

Model framework: fractional order model

The goal of this part is to create a mathematical model of infectious disease with CFOD in order to investigate its existence and numerical outcomes. As a result of the previous work, we looked at the model (1) by taking fractional order derivative for the considered equations. The qualitative theory of the existence of a solution to the consider model utilising a fixed point technique is the subject of our research. In addition, we establish feasibility and solution bounds. We devised a numerical approach to give the model under consideration a graphical representation of the result. Let us use Caputo fractional differential equations to formulate the $T_S T_E T_I T_A T_H T_R$ compartmental model in a fractional order framework.

$$
\begin{aligned}
{}^{c}_{t_0}D^{a}_{t}T_S(t) &= A - \pi T_S(t)\big(T_I(t) + \kappa T_A(t)\big) + vT_E(t) - \vartheta T_S(t)\\
{}^{c}_{t_0}D^{a}_{t}T_E(t) &= \pi T_S(t)\big(T_I(t) + \kappa T_A(t)\big) - (\sigma + v + \vartheta)T_E(t)\\
{}^{c}_{t_0}D^{a}_{t}T_I(t) &= \eta\sigma T_E(t) - (\psi_1 + \vartheta + \vartheta_1 + \xi_1)T_I(t)\\
{}^{c}_{t_0}D^{a}_{t}T_A(t) &= (1-\eta)\sigma T_E(t) - (\psi_2 + \vartheta + \vartheta_2 + \xi_2)T_A(t)\\
{}^{c}_{t_0}D^{a}_{t}T_H(t) &= \xi_1 T_I(t) + \xi_2 T_A(t) - (\psi_3 + \vartheta)T_H(t)\\
{}^{c}_{t_0}D^{a}_{t}T_R(t) &= \psi_1 T_I(t) + \psi_2 T_A(t) + \psi_3 T_H(t) - \vartheta T_R(t)
\end{aligned}
\tag{3}
$$

where $0 < a \leq 1$, and ${}^{c}_{t_0}D^{a}_{t}$ is the notation due to Caputo fractional derivative, $t_0 \geq 0$ is the initial time (it is assumed that $t_0 = 0$).

Qualitative properties of solution

Here, we look at how well-posed the fractional order model is mathematically and biologically. We show that the CFOD's solution is bounded and positive as long as a positive initial condition is specified. We also demonstrate the solution to the modified model's existence and uniqueness.

Let $\Theta(t) = (T_S, T_E, T_I, T_A, T_H, T_R)^T$ and $\mathcal{K}(t, \Theta(t)) = (\Psi_i)^T, i = 1, 2, \ldots, 6$ where

$$
\begin{aligned}
\Psi_1 &= A - \pi T_S(t)\big(T_I(t) + \kappa T_A(t)\big) + vT_E(t) - \vartheta T_S(t)\\
\Psi_2 &= \pi T_S(t)\big(T_I(t) + \kappa T_A(t)\big) - (\sigma + v + \vartheta)T_E(t)\\
\Psi_3 &= \eta\sigma T_E(t) - (\psi_1 + \vartheta + \vartheta_1 + \xi_1)T_I(t)\\
\Psi_4 &= (1-\eta)\sigma T_E(t) - (\psi_2 + \vartheta + \vartheta_2 + \xi_2)T_A(t)\\
\Psi_5 &= \xi_1 T_I(t) + \xi_2 T_A(t) - (\psi_3 + \vartheta)T_H(t)\\
\Psi_6 &= \psi_1 T_I(t) + \psi_2 T_A(t) + \psi_3 T_H(t) - \vartheta T_R(t)
\end{aligned}
$$

The dynamical system (3) becomes

$$
{}^{c}_{t_0}D^{a}_{t}\Theta(t) = \mathcal{K}(t, \Theta(t)),\ \Theta(0) = \Theta_0 \geq 0,\ t \in [0, f],\ a \in (0, 1]
\tag{4}
$$

Here $\Theta(0) \geq 0$ is to be depicted component-wise. Model(3), which is similar to fractional differential equation (4), its integral representation is

$$
\begin{aligned}
\Theta(t) &= \Theta_0 + \mathcal{J}^{a}_{0+}\mathcal{K}(t, \Theta(t))\\
&= \Theta_0 + \frac{1}{\Gamma(a)}\int_0^t (t - \varrho)^{a-1}\mathcal{K}(\varrho, \Theta(\varrho))d\varrho
\end{aligned}
\tag{5}
$$

For analysing model (3), let $\mu = C([0, f]; \mathbb{R})$ represents the Banach space of all continuous functions from $[0, f]$ to $\mathbb{R}$ with the norm

$$
\|\Theta\|_{\mu} = \sup_{t \in [0,f]} (|\Theta(t)|)
$$

where

$$|\Theta(t)| = |T_S(t)| + |T_E(t)| + |T_I(t)| + |T_A(t)| + |T_H(t)| + |T_R(t)|$$

. Specify that $T_S, T_E, T_I, T_A, T_H, T_R \in C([0,f];\mathbb{R})$. Additionally, we define the operator $\mathcal{G}: \mu \to \mu$ by

$$(\mathcal{G}\Theta)(t) = \Theta_0 + \frac{1}{\Gamma(a)}\int_0^t (t-\varrho)^{a-1}\mathcal{K}(\varrho,\Theta(\varrho))d\varrho \qquad (6)$$

The continuity of $\mathcal{K}$ is obvious implies $\mathcal{G}$ is well-defined.

Positivity and boundedness of solution

The solution of the CFOD's model is found to be positive and bounded at all times in order for it to be biologically well-posed. The sequel establishes these characteristics.

Theorem 4.1 *The set*

$$\Delta = \left\{(T_S, T_E, T_I, T_A, T_R) \in \mathbb{R}_+^5 | 0 \le T_S, T_E, T_I, T_A, T_R \le \frac{A}{\vartheta}\right\}$$

is a positively invariant and the attraction region for system (3).

Proof Let $N(t) = T_S + T_E + T_I + T_A + T_R$.

Then ${}_{t_0}^{c}D_t^a N(t) \le A - \vartheta N(t)$. Using Laplace transform,

$$\begin{aligned} N(t) &\le At^a E_{a,a+1}(-\vartheta t^a) + N(0)E_{a,1}(-\vartheta t^a) \\ &\le \frac{A}{\vartheta}\left(1 - E_{a,1}(-\vartheta t^a)\right) + N(0)E_{a,1}(-\vartheta t^a) \end{aligned}$$

Since $E_{a,1}(-\vartheta t^a) \in [0,1]$ and $N(0) \le \frac{A}{\vartheta}$, we get $N(t) \le \frac{A}{\vartheta}$. Thus, Δ is a positively invariant set, and all initial solutions remain in Δ for all $t > 0$. □

Existence of unique and uniformly stable solution

Theorem 4.2 *Let* $\widehat{\Theta}(t) = (\widehat{T}_S, \widehat{T}_E, \widehat{T}_I, \widehat{T}_A, \widehat{T}_R)^T$. *The function* $\mathcal{K}(t,\Theta(t)) = (\psi_i)^T, i = 1,2,\ldots,6$ *defined above satisfies*

$$\left\|\mathcal{K}(t,\Theta(t)) - \mathcal{K}\left(t,\widehat{\Theta}(t)\right)\right\|_\mu \le \omega\|\Theta - \widehat{\Theta}\|_\mu$$

for some $\omega > 0$

Proof By the first set of $\mathcal{K}$, notice that $\left|\psi_1(t,\Theta(t)) - \psi_1(t,\widehat{\Theta}(t))\right|$

$$\begin{aligned} &= \Big| - \pi\big(T_S(t)T_I(t) - \widehat{T}_S(t)\widehat{T}_I(t)\big) \\ &\quad - \pi\kappa\big(T_S(t)T_A(t) - \widehat{T}_S(t)\widehat{T}_A(t)\big) + v\big(T_E(t) - \widehat{T}_E(t)\big) \\ &\quad - \vartheta\big(T_S(t) - \widehat{T}_S(t)\big)\Big| \\ &\le \pi\left|T_S(t)T_I(t) - \widehat{T}_S(t)\widehat{T}_I(t)\right| \\ &\quad + \pi\kappa\left|T_S(t)T_A(t) - \widehat{T}_S(t)\widehat{T}_A(t)\right| + v\left|T_E(t) - \widehat{T}_E(t)\right| \\ &\quad + \vartheta\left|T_S(t) - \widehat{T}_S(t)\right| \\ &\le \big(\vartheta + \pi\left|T_I(t)\right| \\ &\quad + \pi\kappa\left|T_A(t)\right|\big)\left|T_S(t) - \widehat{T}_S(t)\right| + v\left|T_E(t) - \widehat{T}_E(t)\right| \\ &\quad + \pi\left|\widehat{T}_S(t)\right|\left|T_I(t) - \widehat{T}_I(t)\right| \\ &\quad + \pi\kappa\left|\widehat{T}_S(t)\right|\left|T_A(t)\right. \\ &\quad \left. - \widehat{T}_A(t)\right| \\ &\le \omega_1\Big(\left|T_S(t) - \widehat{T}_S(t)\right| + \left|T_E(t) - \widehat{T}_E(t)\right| + \left|T_I(t)\right. \\ &\quad \left. - \widehat{T}_I(t)\right| + \left|T_A(t) - \widehat{T}_A(t)\right| + \left|T_R(t) - \widehat{T}_R(t)\right|\Big) \end{aligned}$$

where,

$$\omega_1 = (\vartheta + v) + \max_{t\in[0,f]}\Big(\pi\left|T_I(t)\right| + \pi\kappa\left|T_A(t)\right| + \pi\left|\widehat{T}_S(t)\right| + \pi\kappa\left|\widehat{T}_S(t)\right|\Big)$$

Similarly,

$$\begin{aligned} &\left|\Psi_2(t,\Theta(t)) - \Psi_2(t,\widehat{\Theta}(t))\right| \\ &\le \omega_2\Big(\left|T_S(t) - \widehat{T}_S(t)\right| + \left|T_E(t) - \widehat{T}_E(t)\right| \\ &\quad + \left|T_I(t) - \widehat{T}_I(t)\right| + \left|T_A(t) - \widehat{T}_A(t)\right|\Big) \\ &\left|\Psi_3(t,\Theta(t)) - \Psi_3(t,\widehat{\Theta}(t))\right| \\ &\le \omega_3\Big(\left|T_E(t) - \widehat{T}_E(t)\right| + \left|T_I(t) - \widehat{T}_I(t)\right|\Big) \\ &\left|\Psi_4(t,\Theta(t)) - \Psi_4(t,\widehat{\Theta}(t))\right| \\ &\le \omega_4\Big(\left|T_E(t) - \widehat{T}_E(t)\right| + \left|T_A(t) - \widehat{T}_A(t)\right|\Big) \\ &\left|\Psi_5(t,\Theta(t)) - \Psi_5(t,\widehat{\Theta}(t))\right| \\ &\le \omega_5\Big(\left|T_I(t) - \widehat{T}_I(t)\right| + \left|T_A(t) - \widehat{T}_A(t)\right| + \left|T_H(t) - \widehat{T}_H(t)\right|\Big) \\ &\left|\Psi_6(t,\Theta(t)) - \Psi_6(t,\widehat{\Theta}(t))\right| \\ &\le \omega_6\Big(\left|T_I(t) - \widehat{T}_I(t)\right| \\ &\quad + \left|T_A(t) - \widehat{T}_A(t)\right| + \left|T_H(t) - \widehat{T}_H(t)\right| + \left|T_R(t) - \widehat{T}_R(t)\right|\Big) \end{aligned}$$

where,

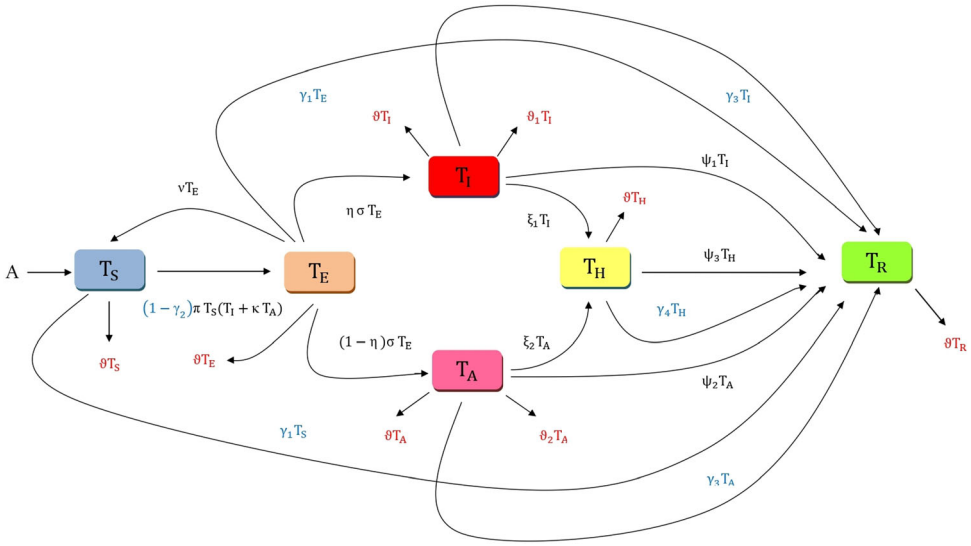

Fig. 3 Schematic Diagram for the Optimal Control Dynamics of Disease

$$\omega_2 = (\sigma + \nu + \vartheta) + \max_{t\in[0,f]}\left(\pi|T_I(t)| + \pi\kappa|T_A(t)| + \pi|\widehat{T}_S(t)| + \pi\kappa|\widehat{T}_S(t)|\right)$$

$$\omega_3 = (\eta\sigma + \psi_1 + \vartheta + \vartheta_1 + \xi_1),\ \omega_4 = |(1-\eta)|\sigma + \psi_2 + \vartheta + \vartheta_2 + \xi_2,$$

$$\omega_5 = \xi_1 + \xi_2 + \psi_3 + \vartheta,\ \omega_6 = \psi_1 + \psi_2 + \psi_3 + \vartheta$$

Then,

$$\|\mathcal{K}(t,\Theta(t)) - \mathcal{K}(t,\widehat{\Theta}(t))\|_\mu = \sup_{t\in[0,f]}\sum_{k=1}^{6}\left|\psi_k(t,\Theta(t)) - \psi_k(t,\widehat{\Theta}(t))\right| \le \omega\|\Theta - \widehat{\Theta}\|_\mu$$

where $\omega = \omega_1 + \omega_2 + \omega_3 + \omega_4 + \omega_5$ □

Theorem 4.3 *Let Theorem 4.2 holds and* $\Xi = \dfrac{f^a}{\Gamma(a)}$. *If* $\Xi\omega < 1$ *then there exists a unique solution of model (3) on* $[0, f]$ *which is uniformly Lyapunov stable.*

Proof The function $\mathcal{K} : [0,f] \times \mathbb{R}_+^6 \to \mathbb{R}_+^6$ is obviously continuous on its domain. As a result of Lin (2007), the existence of solution to (3) follows.

The Principle of Banach contraction mapping on operator $\mathcal{G}$ defined in (6) is used for uniqueness. We prove that $\mathcal{G}$ is contraction and self map. From definition, $\sup_{t\in[0,f]}|\mathcal{K}(\varrho,0)| = A$. Define $\mathcal{Z} > \dfrac{|\Theta_0| + \Xi f^a}{1 - \Xi\omega}$ and a closed convex set $Q_\mathcal{Z} = \left\{\Theta \in \mu : |\Theta|_\mu \le \mathcal{Z}\right\}$. It suffices to show that $\mathcal{G}Q_\mathcal{Z} \subseteq Q_\mathcal{Z}$ for self map property. So, let $\Theta \in Q_\mathcal{Z}$, then

$$\begin{aligned}
\|\mathcal{G}\Theta\|_\mu &= \sup_{t\in[0,f]}\left\{\left|\Theta_0 + \frac{1}{\Gamma(a)}\int_0^t (t-\varrho)^{a-1}\mathcal{K}(\varrho,\Theta(\varrho))d\varrho\right|\right\}\\
&\le |\Theta_0| + \frac{1}{\Gamma(a)}\sup_{t\in[0,f]}\left\{\int_0^t (t-\varrho)^{a-1}\left(|\mathcal{K}(\varrho,\Theta(\varrho)) - \mathcal{K}(\varrho,0)| + |\mathcal{K}(\varrho,0)|\right)d\varrho\right\}\\
&\le |\Theta_0| + \frac{1}{\Gamma(a)}\sup_{t\in[0,f]}\left\{\int_0^t (t-\varrho)^{a-1}\left(|\mathcal{K}(\varrho,\Theta(\varrho)) - \mathcal{K}(\varrho,0)|_\mu + |\mathcal{K}(\varrho,0)|_\mu\right)d\varrho\right\}\\
&\le |\Theta_0| + \frac{\omega\|\Theta\|_\mu + A}{\Gamma(a)}\sup_{t\in[0,f]}\left\{\int_0^t (t-\varrho)^{a-1}d\varrho\right\}\\
&\le |\Theta_0| + \frac{\omega\mathcal{Z} + A}{\Gamma(a)}\sup_{t\in[0,f]}\left\{\int_0^t (t-\varrho)^{a-1}d\varrho\right\}\\
&= |\Theta_0| + \frac{\omega\mathcal{Z} + A}{\Gamma(a)}f^a\\
&= |\Theta_0| + \Xi(\omega\mathcal{Z} + A)\\
&\le \mathcal{Z}
\end{aligned}$$

Therefore $\mathcal{G}\Theta \subseteq Q_\mathcal{Z}$. Hence $\mathcal{G}$ is a self-map. Now we claim that $\mathcal{G}$ is a contraction. Consider Θ and $\widehat{\Theta} \in \mu$ satisfy (4). From Theorem 4.2 we get,

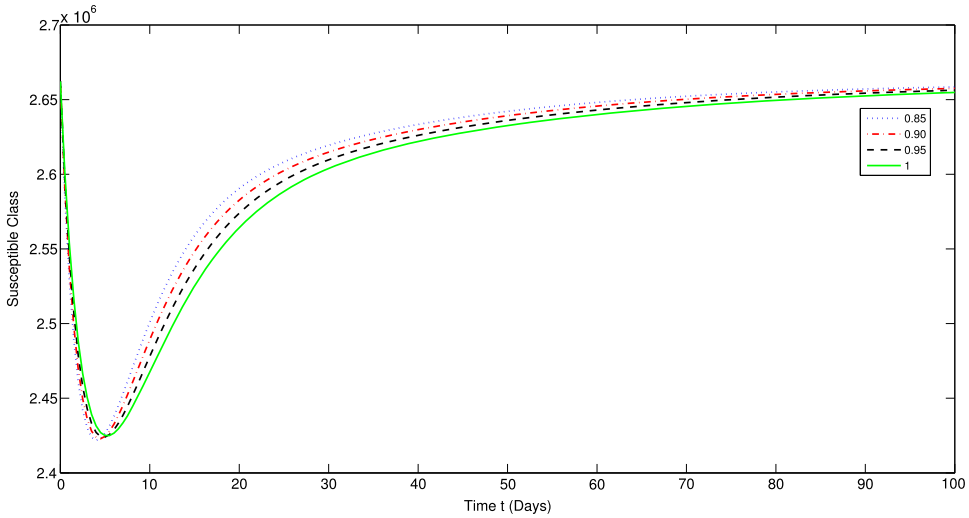

Fig. 4 Dynamical behaviour of susceptible class at various fractional order of a

$$
\begin{aligned}
&\left|\mathcal{G}\Theta - \mathcal{G}\widehat{\Theta}\right|_{\mu} = \\
&\sup_{t\in[0,f]}\left\{\left|\mathcal{G}\Theta(t) - \mathcal{G}\widehat{\Theta}(t)\right|\right\} \\
&= \frac{1}{\Gamma(a)}\sup_{t\in[0,f]}\left\{\int_0^t (t-\varrho)^{a-1}\left|\mathcal{K}(\varrho,\Theta(\varrho)) - \mathcal{K}(\varrho,\widehat{\Theta}(\varrho))\right|d\varrho\right\} \\
&\leq \frac{\omega}{\Gamma(a)}\sup_{t\in[0,f]}\left\{\int_0^t (t-\varrho)^{a-1}\left|\Theta(\varrho) - \widehat{\Theta}(\varrho)\right|d\varrho\right\} \\
&\leq \Xi\omega\left|\Theta(\varrho) - \widehat{\Theta}(\varrho)\right|_{\mu}
\end{aligned}
$$

Thus if $\Xi\omega < 1$ then $\mathcal{G}$ is a contraction mapping, then by the principle of Banach contraction mapping, $\mathcal{G}$ has a unique fixed point on $[0, f]$ which is solution of (3). From El-Sayed (2010) the solution is Uniformly Lyapunov stable.□

Optimal control

Motivated by the work of Baba and Bilgehan (2021), research has utilized fractional-order mathematical models with optimal control strategies to understand and mitigate the spread of infectious diseases. These studies emphasize the effectiveness of combining preventive measures, such as awareness campaigns, and treatment protocols to reduce disease transmission and improve public health outcomes. We enhance our model in this part by including four time-dependent control measures, namely $\gamma_1, \gamma_2, \gamma_3$ and γ_4. Let us define a control function $\gamma = (\gamma_1, \gamma_2, \gamma_3, \gamma_4)$, where γ_1 is the control for the variation in the behaviour of the susceptible and exposed population by following all health care measures and suggestions. γ_2 refers to the application of all pretreatments to an infected individual, whether exposed or latent, γ_3 is a control feature that increases the potency of treatment for both symptomatic and asymptomatic patients and γ_4 is the control for the variation in the behaviour of hospitalized class who gets extra attention and care. The model's optimal control dynamics is depicted in the diagram below (see Fig. 3).

$$
\begin{aligned}
{}^{c}_{t_0}D^{a}_{t}T_S(t) =& A - (1-\gamma_2)\pi T_S(t)\big(T_I(t) \\
&+ \kappa T_A(t)\big) + \nu T_E(t) - (\vartheta + \gamma_1)T_S(t) \\
{}^{c}_{t_0}D^{a}_{t}T_E(t) =& (1-\gamma_2)\pi T_S(t)\big(T_I(t) \\
&+ \kappa T_A(t)\big) - (\sigma + \nu + \vartheta + \gamma_1)T_E(t) \\
{}^{c}_{t_0}D^{a}_{t}T_I(t) =& \eta\sigma T_E(t) - (\psi_1 + \vartheta + \vartheta_1 \\
&+ \xi_1 + \gamma_3)T_I(t) \\
{}^{c}_{t_0}D^{a}_{t}T_A(t) =& (1-\eta)\sigma T_E(t) - (\psi_2 + \vartheta + \vartheta_2 + \xi_2 + \gamma_3)T_A(t) \\
{}^{c}_{t_0}D^{a}_{t}T_H(t) =& \xi_1 T_I(t) + \xi_2 T_A(t) - (\psi_3 + \vartheta + \gamma_4)T_H(t) \\
{}^{c}_{t_0}D^{a}_{t}T_R(t) =& (\psi_1 + \gamma_3)T_I(t) + (\psi_2 + \gamma_3)T_A(t) \\
&+ \gamma_1 T_S(t) + \gamma_1 T_E(t) + (\psi_3 + \gamma_4)T_H(t) - \vartheta T_R(t)
\end{aligned}
\tag{7}
$$

To analyse the state model (7), the optimal control problem (OCP) is established along-with the set of acceptable control function

$$
\begin{aligned}
\varpi = \big\{&(\gamma_1, \gamma_2, \gamma_3, \gamma_4)|\gamma_i : [0, t_f] \\
&\to [0, \infty) \text{ Lebesgue measurable, } i = 1, 2, 3, 4\big\}
\end{aligned}
$$

. Then we define an objective functional,

$$
\begin{aligned}
\mathcal{J}(\gamma_1, \gamma_2, \gamma_3, \gamma_4) = \int_0^{t_f} \Big(&\mathcal{C}_1 T_E(t) + \mathcal{C}_2 T_I(t) + \mathcal{C}_3 T_A(t) \\
&+ \frac{1}{2}\left(c_1\gamma_1^2 + c_2\gamma_2^2 + c_3\gamma_3^2 + c_4\gamma_4^2\right)\Big)dt
\end{aligned}
\tag{8}
$$

where the positive weights $\mathcal{C}_i : i = 1, 2, 3,$ and $c_i : i = 1, 2, 3, 4$ are used to balance the control factors. Our goal is to reduce the infected human populations at the cost of

reducing control $\gamma_1, \gamma_2, \gamma_3, \gamma_4$. Consequently, we find an optimal control $\gamma_1^\star, \gamma_2^\star, \gamma_3^\star, \gamma_4^\star$, such that

$$\mathcal{J}(\gamma_1^\star, \gamma_2^\star, \gamma_3^\star, \gamma_4^\star) = \min_{\gamma_1,\gamma_2,\gamma_3,\gamma_4} \left\{ \mathcal{J}(\gamma_1, \gamma_2, \gamma_3, \gamma_4) | \gamma_1, \gamma_2, \gamma_3, \gamma_4 \in \varpi \right\} \tag{9}$$

The necessary conditions that must be satisfied by an optimal control can be derived from the Pontryagin's Minimum Principle (PMP). This principle converts (7) and (3) into a problem of point-wise minimizing a Hamiltonian $\mathcal{M}$ corresponds to $(\gamma_1, \gamma_2, \gamma_3, \gamma_4)$ stated as follows:

$$\begin{aligned}
\mathcal{M} &= \mathcal{C}_1 T_E + \mathcal{C}_2 T_I + \mathcal{C}_3 T_A \\
&+ \frac{1}{2}\left(c_1\gamma_1^2 + c_2\gamma_2^2 + c_3\gamma_3^2 + c_4\gamma_4^2\right) + \zeta_{T_S}\Big\{A - (1-\gamma_2)\pi T_S(t)\big(T_I(t) + \kappa T_A(t)\big) \\
&+ \nu T_E(t) - (\vartheta + \gamma_1)T_S(t)\Big\} + \zeta_{T_E}\Big\{(1-\gamma_2)\pi T_S(t)\big(T_I(t) \\
&+ \kappa T_A(t)\big) - (\sigma + \nu + \vartheta + \gamma_1)T_E(t)\Big\} \\
&+ \zeta_{T_I}\Big\{\eta\sigma T_E(t) - (\psi_1 + \vartheta + \vartheta_1 \\
&+ \xi_1 + \gamma_3)T_I(t)\Big\} \\
&+ \zeta_{T_A}\Big\{(1-\eta)\sigma T_E(t) - (\psi_2 + \vartheta + \vartheta_2 + \xi_2 + \gamma_3)T_A(t)\Big\} \\
&+ \zeta_{T_H}\Big\{\xi_1 T_I(t) + \xi_2 T_A(t) - (\psi_3 + \vartheta \\
&+ \gamma_4)T_H(t)\Big\} + \zeta_{T_R}\Big\{(\psi_1 + \gamma_3)T_I(t) + (\psi_2 + \gamma_3)T_A(t) + \gamma_1 T_S(t) \\
&+ \gamma_1 T_E(t) + (\psi_3 + \gamma_4)T_H(t) - \vartheta T_R(t)\Big\}
\end{aligned}$$

Where, $\zeta_{T_S}, \zeta_{T_E}, \zeta_{T_I}, \zeta_{T_A}, \zeta_{T_H}$ and ζ_{T_R} are adjoint variables or co-state variables

$$\begin{aligned}
&\frac{\partial \mathcal{M}}{\partial T_S} = \zeta_{T_S}\Big\{(1-\gamma_2)\pi\big(T_I(t) \\
&+ \kappa T_A(t)\big) + \vartheta + \gamma_1\Big\} - \zeta_{T_E}\Big\{(1-\gamma_2)\pi\big(T_I(t) + \kappa T_A(t)\big)\Big\} - \zeta_{T_R}\gamma_1 \\
&\frac{\partial \mathcal{M}}{\partial T_E} = -\mathcal{C}_1 - \zeta_{T_S}\nu + \zeta_{T_E}(\sigma + \nu + \vartheta + \gamma_1) \\
&- \zeta_{T_I}\eta\sigma - \zeta_{T_A}(1-\eta)\sigma - \zeta_{T_R}\gamma_1 \\
&\frac{\partial \mathcal{M}}{\partial T_I} = -\mathcal{C}_2 + \zeta_{T_S}(1-\gamma_2)\pi T_S \\
&- \zeta_{T_E}(1-\gamma_2)\pi T_S + \zeta_{T_I}(\psi_1 + \vartheta + \vartheta_1 \\
&+ \xi_1 + \gamma_3) - \xi_1\zeta_{T_H} - (\psi_1 + \gamma_3)\zeta_{T_R} \\
&\frac{\partial \mathcal{M}}{\partial T_A} = -\mathcal{C}_3 + \zeta_{T_S}(1-\gamma_2)\pi \\
&\kappa T_S - \zeta_{T_E}(1-\gamma_2)\pi\kappa T_S + \zeta_{T_A} \\
&(\psi_2 + \vartheta + \vartheta_2 + \xi_2 + \gamma_3) - \xi_2\zeta_{T_H} - (\psi_2 + \gamma_3)\zeta_{T_R} \\
&\frac{\partial \mathcal{M}}{\partial T_H} = \zeta_{T_H}(\psi_3 + \vartheta + \gamma_4) \\
&- \zeta_{T_R}(\psi_3 + \gamma_4) \\
&\frac{\partial \mathcal{M}}{\partial T_R} = \zeta_{T_R}\vartheta
\end{aligned} \tag{10}$$

The transversality conditions are

$$\zeta_{T_S(t_f)} = \zeta_{T_E(t_f)} = \zeta_{T_I(t_f)} = \zeta_{T_A(t_f)} = \zeta_{T_H(t_f)} = \zeta_{T_R(t_f)} = 0$$

. On the interior of the control set, where $0 < \gamma_i < 1$, for $i = 1, 2, 3, 4$.

$$\frac{\partial \mathcal{M}}{\partial \gamma_1} = c_1\gamma_1 - \zeta_{T_S}T_S - \zeta_{T_E}T_E + \zeta_{T_R}T_S + \zeta_{T_R}T_E = 0$$

$$\frac{\partial \mathcal{M}}{\partial \gamma_2} = c_2\gamma_2 + \zeta_{T_S}\pi T_S(T_I + \kappa T_A) - \zeta_{T_E}\pi T_S(T_I + \kappa T_A) = 0$$

$$\frac{\partial \mathcal{M}}{\partial \gamma_3} = c_3\gamma_3 - \zeta_{T_A}T_A - \zeta_{T_I}T_I + \zeta_{T_R}T_I + \zeta_{T_R}T_A = 0$$

$$\frac{\partial \mathcal{M}}{\partial \gamma_4} = c_4\gamma_4 - \zeta_{T_H}T_H + \zeta_{T_R}T_H = 0$$

From where,

$$\gamma_1 = \frac{T_S(\zeta_{T_S} - \zeta_{T_R}) + T_E(\zeta_{T_E} - \zeta_{T_R})}{c_1}$$

$$\gamma_2 = \frac{\pi T_S(T_I + \kappa T_A)(\zeta_{T_E} - \zeta_{T_S})}{c_2}$$

$$\gamma_3 = \frac{T_A(\zeta_{T_A} - \zeta_{T_R}) + T_I(\zeta_{T_I} - \zeta_{T_R})}{c_3}$$

$$\gamma_4 = \frac{T_H(\zeta_{T_H} - \zeta_{T_R})}{c_4}$$

Theorem 5.1 *The control parameters* $(\gamma_1^\star, \gamma_2^\star, \gamma_3^\star, \gamma_4^\star)$, *that minimizes* $\mathcal{J}(\gamma_1, \gamma_2, \gamma_3, \gamma_4)$ *over* ϖ *are given by*:

$$\gamma_1^\star = \max\left\{0, \min\left[1, \frac{T_S(\zeta_{T_S}-\zeta_{T_R})+T_E(\zeta_{T_E}-\zeta_{T_R})}{c_1}\right]\right\}$$
$$\gamma_2^\star = \max\left\{0, \min\left[1, \frac{\pi T_S(T_I+\kappa T_A)(\zeta_{T_E}-\zeta_{T_S})}{c_2}\right]\right\}$$
$$\gamma_3^\star = \max\left\{0, \min\left[1, \frac{T_A(\zeta_{T_A}-\zeta_{T_R})+T_I(\zeta_{T_I}-\zeta_{T_R})}{c_3}\right]\right\}$$
$$\gamma_4^\star = \max\left\{0, \min\left[1, \frac{T_H(\zeta_{T_H}-\zeta_{T_R})}{c_4}\right]\right\} \tag{11}$$

where $\zeta_{T_S}, \zeta_{T_E}, \zeta_{T_I}, \zeta_{T_A}$ and ζ_{T_R} are adjoint variables. *Transversality conditions are* $\zeta_{T_S(t_f)} = \zeta_{T_E(t_f)} = \zeta_{T_I(t_f)} = \zeta_{T_A(t_f)} = \zeta_{T_R(t_f)} = 0$.

$$\gamma_1^\star = \begin{cases} 0 \text{ if } \gamma_1 \le 0 \\ \gamma_1 \text{ if } 0<\gamma_1<1 \\ 1 \text{ if } \gamma_1 \ge 1 \end{cases}, \quad \gamma_2^\star = \begin{cases} 0 \text{ if } \gamma_2 \le 0 \\ \gamma_2 \text{ if } 0<\gamma_2<1 \\ 1 \text{ if } \gamma_2 \ge 1 \end{cases}$$
$$\gamma_3^\star = \begin{cases} 0 \text{ if } \gamma_3 \le 0 \\ \gamma_3 \text{ if } 0<\gamma_3<1 \\ 1 \text{ if } \gamma_3 \ge 1 \end{cases}, \quad \gamma_4^\star = \begin{cases} 0 \text{ if } \gamma_3 \le 0 \\ \gamma_4 \text{ if } 0<\gamma_4<1 \\ 1 \text{ if } \gamma_4 \ge 1 \end{cases}$$

Proof The existence of an optimal solution with the corresponding optimal control result can be derived from the convexity of integrand of $\mathcal{J}$ corresponds to control γ_1, γ_2 and γ_3, a priori boundedness of the state solutions, and the Lipschitz property of the state system corresponds to the state variables. Using PMP,

$$\begin{aligned} {}_{t_0}^{c}D_t^a\zeta_{T_S} &= \frac{\partial \mathcal{M}}{\partial T_S}, \; {}_{t_0}^{c}D_t^a\zeta_{T_E} \\ &= \frac{\partial \mathcal{M}}{\partial T_E}, \; {}_{t_0}^{c}D_t^a\zeta_{T_I} = \frac{\partial \mathcal{M}}{\partial T_I}, \; {}_{t_0}^{c}D_t^a\zeta_{T_A} = \frac{\partial \mathcal{M}}{\partial T_A}, \\ {}_{t_0}^{c}D_t^a\zeta_{T_H} &= \frac{\partial \mathcal{M}}{\partial T_H}, \; {}_{t_0}^{c}D_t^a\zeta_{T_R} = \frac{\partial \mathcal{M}}{\partial T_R}, \end{aligned} \tag{12}$$

With $\zeta_{T_S(t_f)} = \zeta_{T_E(t_f)} = \zeta_{T_I(t_f)} = \zeta_{T_A(t_f)} = \zeta_{T_H(t_f)} = \zeta_{T_R(t_f)} = 0$.

The optimality conditions is derived by differentiating Hamiltonian $\mathcal{M}$ corresponds to the control variables γ_1, γ_2 and γ_3,

$$\frac{\partial \mathcal{M}}{\partial \gamma_1} = 0, \; \frac{\partial \mathcal{M}}{\partial \gamma_2} = 0, \; \frac{\partial \mathcal{M}}{\partial \gamma_3} = 0, \; \frac{\partial \mathcal{M}}{\partial \gamma_4} = 0 \tag{13}$$

The adjoint system (10) and transversality conditions is derived by solving (11), whereas optimal control pair (12) is followed by optimality condition (13). □

Numerical algorithm and discussion

We must assess approximate solutions of the model (3) under CFOD in this section of the article. The numerical simulations are then obtained using the described method. To do this, we use the CFOD to create a numerical technique for simulating our model (3). The fractional-order differential equations in this study are approximated using the Modified Euler's Method (MEM). This approach was selected because of its effectiveness in handling fractional-order systems and its computing efficiency. When it comes to capturing the long-term memory effects that are typical of fractional-order models, MEM is very helpful.

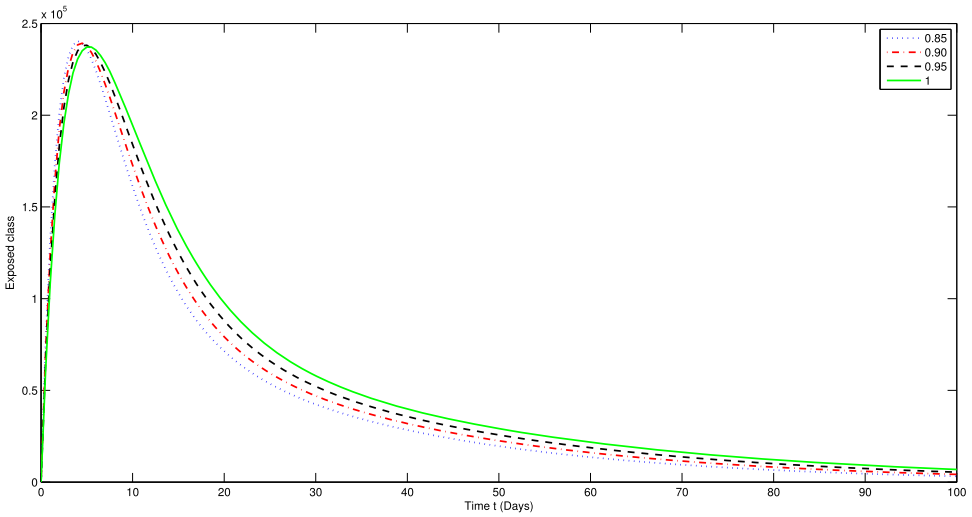

Fig. 5 Dynamical behaviour of exposed class at various fractional order of a

General algorithm

For our examined model (3), we expand Euler's numerical technique. The above-mentioned model may be written as follows:

$$
\begin{aligned}
&{}_{t_0}^{c}D_t^a T_S(t) = \Psi(T_S, T_E, T_I, T_A, T_H, T_R)\\
&= A - \pi T_S(t)\big(T_I(t) + \kappa T_A(t)\big) + \nu T_E(t) - \vartheta T_S(t)\\
&{}_{t_0}^{c}D_t^a T_E(t) = \Psi(T_S, T_E, T_I, T_A, T_H, T_R)\\
&= \pi T_S(t)\big(T_I(t) + \kappa T_A(t)\big) - (\sigma + \nu + \vartheta)T_E(t)\\
&{}_{t_0}^{c}D_t^a T_I(t) = \Psi(T_S, T_E, T_I, T_A, T_H, T_R)\\
&= \eta\sigma T_E(t) - (\psi_1 + \vartheta + \vartheta_1 + \xi_1)T_I(t)\\
&{}_{t_0}^{c}D_t^a T_A(t) = \Psi(T_S, T_E, T_I, T_A, T_H, T_R)\\
&= (1-\eta)\sigma T_E(t) - (\psi_2 + \vartheta + \vartheta_2 + \xi_2)T_A(t)\\
&{}_{t_0}^{c}D_t^a T_H(t) =\\
&\Psi(T_S, T_E, T_I, T_A, T_H, T_R) = \xi_1 T_I(t) + \xi_2 T_A(t)\\
&-(\psi_3 + \vartheta)T_H(t)\\
&{}_{t_0}^{c}D_t^a T_R(t)\\
=&\Psi(T_S, T_E, T_I, T_A, T_H, T_R) = \psi_1 T_I(t)\\
&+ \psi_2 T_A(t) + \psi_3 T_H(t) - \vartheta T_R(t)
\end{aligned}
\tag{14}
$$

Let $\wp$ be the solution interval for (14). We subdivide the interval $\wp$ into p subintervals $[t_f, t_{f+1}]$ with uniform width $h = \frac{T}{m}$ via using the nodes $t_f = fh$, for $f = 0, 1, \ldots, m$. Let $T_S(t), T_E(t), T_I(t), T_A(t), T_H(t), T_R(t), {}_{t_0}^{c}D_t^a T_S(t), {}_{t_0}^{c}D_t^a T_E(t), {}_{t_0}^{c}D_t^a T_I(t), {}_{t_0}^{c}D_t^a T_A(t), {}_{t_0}^{c}D_t^a T_H(t), {}_{t_0}^{c}D_t^a T_R(t)$, up to higher order are continuous on $\wp$. To expression for t_1 has become as expressed below by doing MEM about $t_0 = 0$ in the considered model (14) provided value k for each t.

$$
\begin{aligned}
T_S(t_1) =& T_S(t_0) + \Psi(T_S(t_0), T_E(t_0), T_I(t_0), T_A(t_0),\\
& T_H(t_0), T_R(t_0))\frac{t^a}{\Gamma(a+1)} + {}_{t_0}^{c}D_t^{2a} T_S(t)|_{t=k}\frac{t^{2a}}{\Gamma(2a+1)}\\
T_E(t_1) =& T_E(t_0) + \Psi(T_S(t_0), T_E(t_0), T_I(t_0), T_A(t_0),\\
& T_H(t_0), T_R(t_0))\frac{t^a}{\Gamma(a+1)} + {}_{t_0}^{c}D_t^{2a} T_E(t)|_{t=k}\frac{t^{2a}}{\Gamma(2a+1)}\\
T_I(t_1) =& T_I(t_0) + \Psi(T_S(t_0), T_E(t_0), T_I(t_0), T_A(t_0),\\
& T_H(t_0), T_R(t_0))\frac{t^a}{\Gamma(a+1)} + {}_{t_0}^{c}D_t^{2a} T_I(t)|_{t=k}\frac{t^{2a}}{\Gamma(2a+1)}\\
T_A(t_1) =& T_A(t_0) + \Psi(T_S(t_0), T_E(t_0), T_I(t_0), T_A(t_0),\\
& T_H(t_0), T_R(t_0))\frac{t^a}{\Gamma(a+1)} + {}_{t_0}^{c}D_t^{2a} T_A(t)|_{t=k}\frac{t^{2a}}{\Gamma(2a+1)}\\
T_H(t_1) =& T_H(t_0) + \Psi(T_S(t_0), T_E(t_0), T_I(t_0), T_A(t_0),\\
& T_H(t_0), T_R(t_0))\frac{t^a}{\Gamma(a+1)} + {}_{t_0}^{c}D_t^{2a} T_H(t)|_{t=k}\frac{t^{2a}}{\Gamma(2a+1)}\\
T_R(t_1) =& T_R(t_0) + \Psi(T_S(t_0), T_E(t_0), T_I(t_0), T_A(t_0), T_H(t_0), T_R(t_0))\\
& \frac{t^a}{\Gamma(a+1)} + {}_{t_0}^{c}D_t^{2a} T_R(t)|_{t=k}\frac{t^{2a}}{\Gamma(2a+1)}
\end{aligned}
\tag{15}
$$

If we choose a small enough step size h, ignore the second-order term involving h^{2a} and obtain the following results from (15):

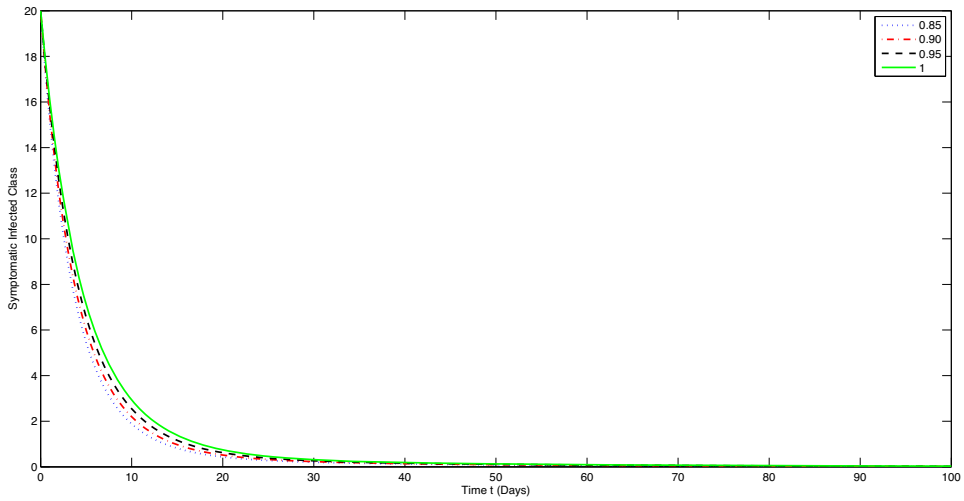

Fig. 6 Dynamical behaviour of symptomatic infected class at various fractional order of a

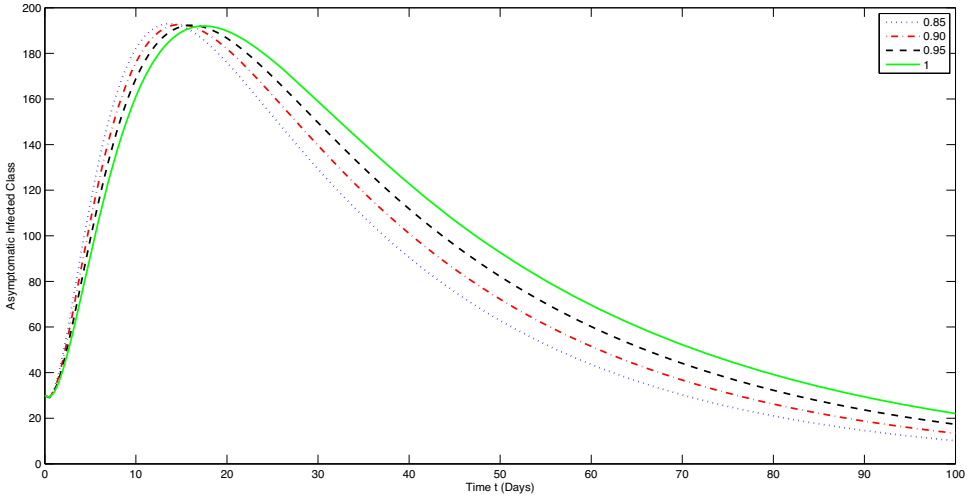

Fig. 7 Dynamical behaviour of asymptomatic infected class at various fractional order of a

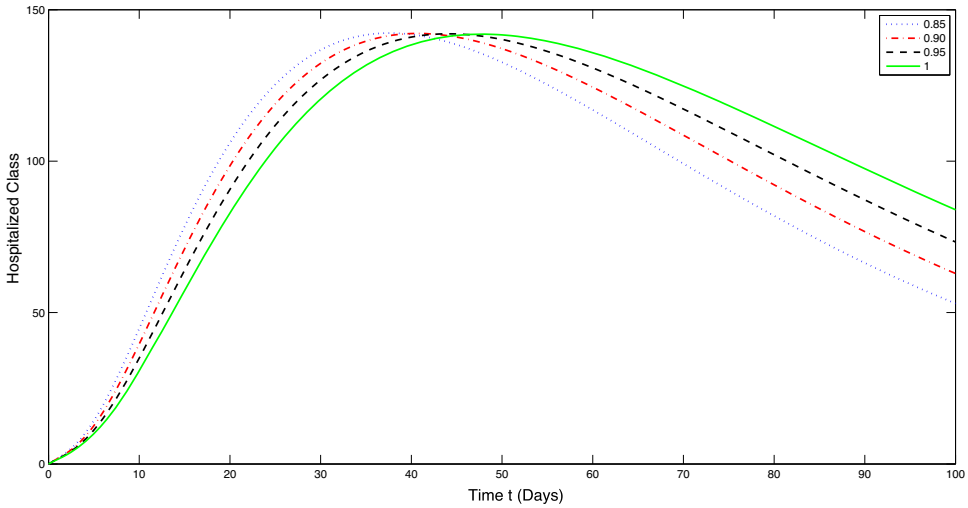

Fig. 8 Dynamical behaviour of hospitalized class at various fractional order of a

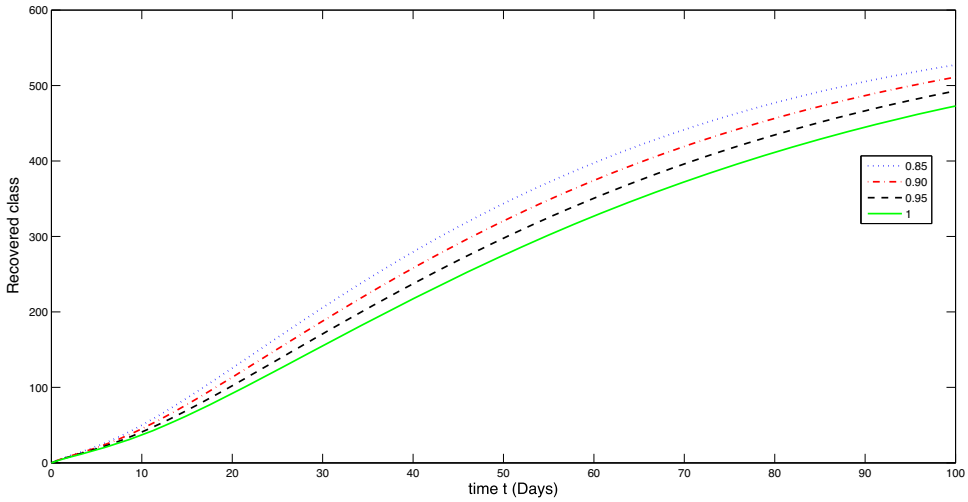

Fig. 9 Dynamical behaviour of recovered class at various fractional order of a

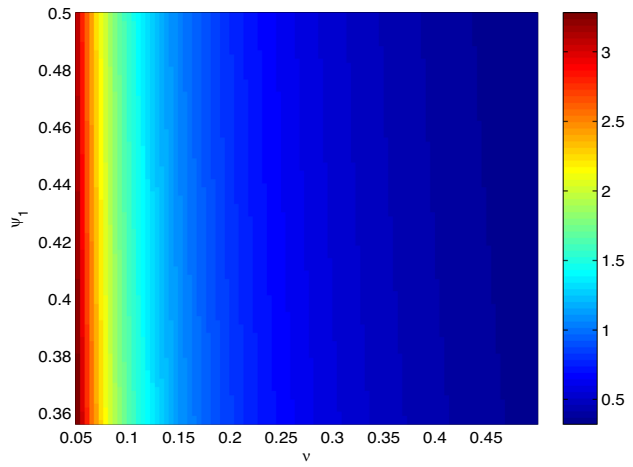

Fig. 10 The contour plot of $\mathcal{R}_0$ in terms of ν and ψ_1

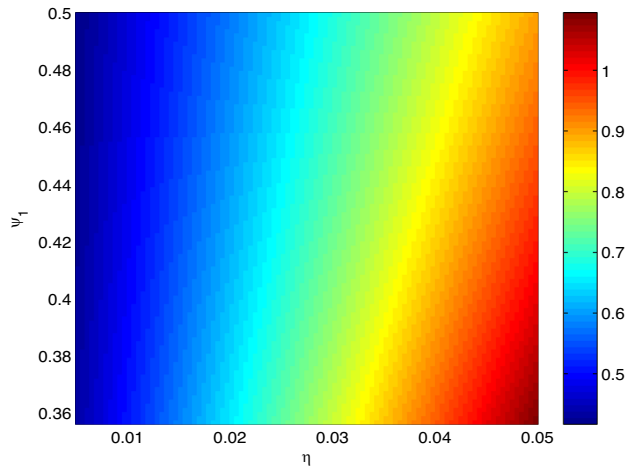

Fig. 11 The contour plot of $\mathcal{R}_0$ in terms of η and ψ_1

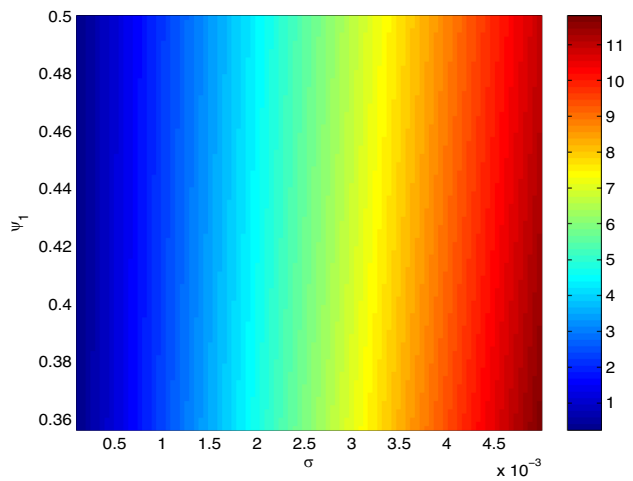

Fig. 12 The contour plot of $\mathcal{R}_0$ in terms of σ and ψ_1

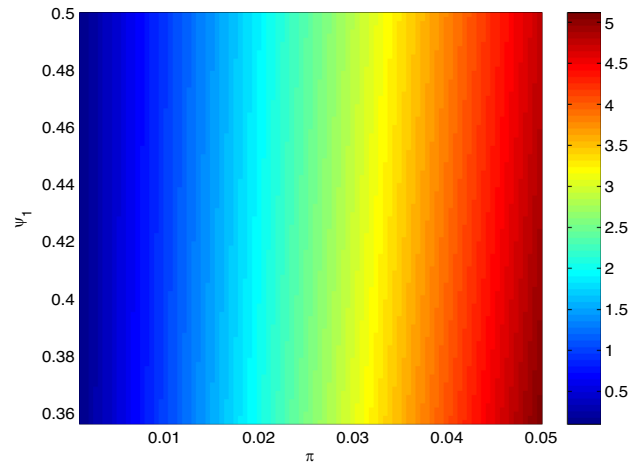

Fig. 13 The contour plot of $\mathcal{R}_0$ in terms of π and ψ_1

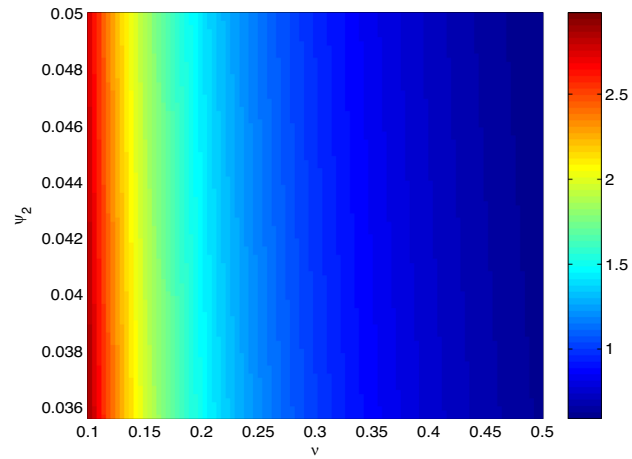

Fig. 14 The contour plot of $\mathcal{R}_0$ in terms of ν and ψ_2

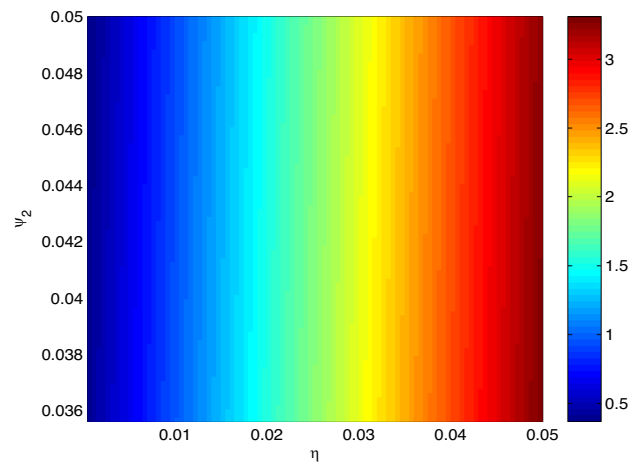

Fig. 15 The contour plot of $\mathcal{R}_0$ in terms of η and ψ_2

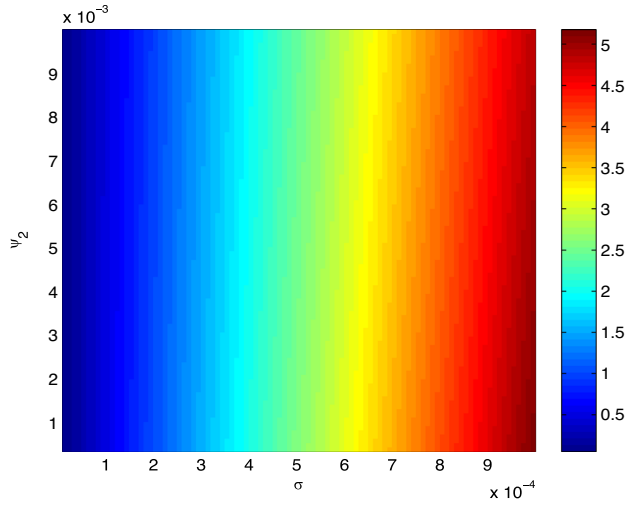

Fig. 16 The contour plot of $\mathcal{R}_0$ in terms of σ and ψ_6

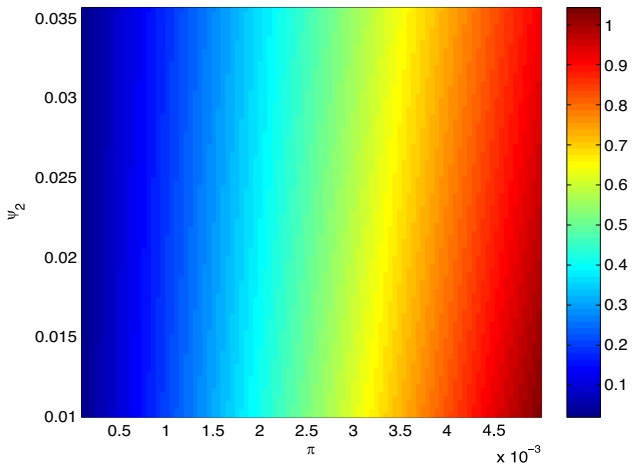

Fig. 17 The contour plot of $\mathcal{R}_0$ in terms of π and ψ_2

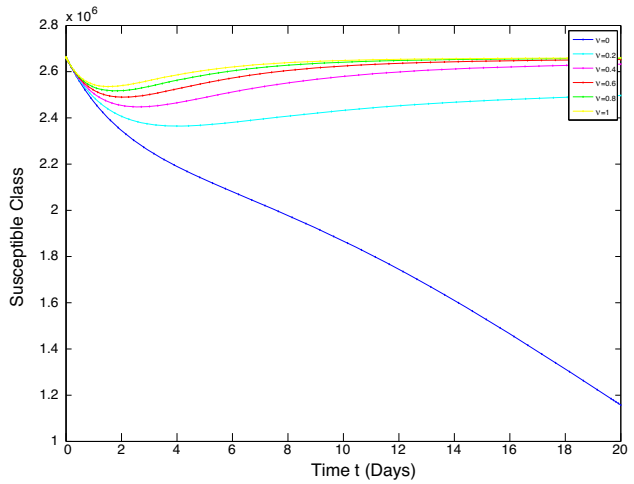

Fig. 18 Impact of v on susceptible class

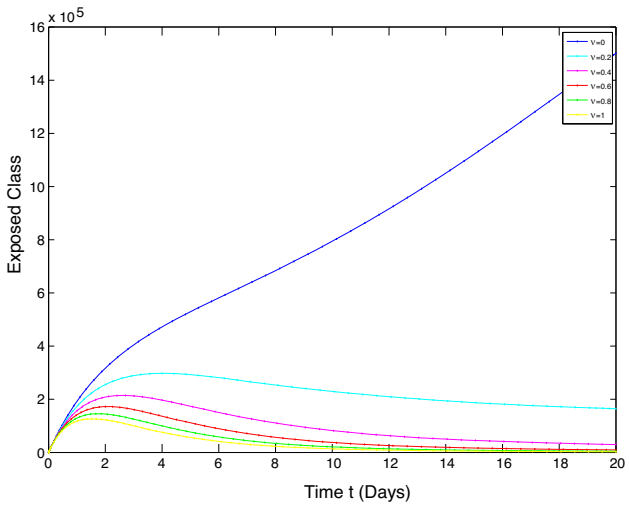

Fig. 19 Impact of v on exposed class

$$
\begin{aligned}
T_S(t_1) =& T_S(t_0) + \Psi(T_S(t_0), T_E(t_0), T_I(t_0), \\
& T_A(t_0), T_H(t_0), T_R(t_0)) \frac{t^a}{\Gamma(a+1)} \\
T_E(t_1) =& T_E(t_0) + \Psi(T_S(t_0), T_E(t_0), T_I(t_0), \\
& T_A(t_0), T_H(t_0), T_R(t_0)) \frac{t^a}{\Gamma(a+1)} \\
T_I(t_1) =& T_I(t_0) + \Psi(T_S(t_0), T_E(t_0), T_I(t_0), \\
& T_A(t_0), T_H(t_0), T_R(t_0)) \frac{t^a}{\Gamma(a+1)} \\
T_A(t_1) =& T_A(t_0) + \Psi(T_S(t_0), T_E(t_0), T_I(t_0), \\
& T_A(t_0), T_H(t_0), T_R(t_0)) \frac{t^a}{\Gamma(a+1)} \\
T_H(t_1) =& T_H(t_0) + \Psi(T_S(t_0), T_E(t_0), T_I(t_0), \\
& T_A(t_0), T_H(t_0), T_R(t_0)) \frac{t^a}{\Gamma(a+1)} \\
T_R(t_1) =& T_R(t_0) + \Psi(T_S(t_0), T_E(t_0), T_I(t_0), \\
& T_A(t_0), T_H(t_0), T_R(t_0)) \frac{t^a}{\Gamma(a+1)}
\end{aligned}
\tag{16}
$$

In the same way, a general formula is established at $t_{f+1} = t_f + h$ as follows:

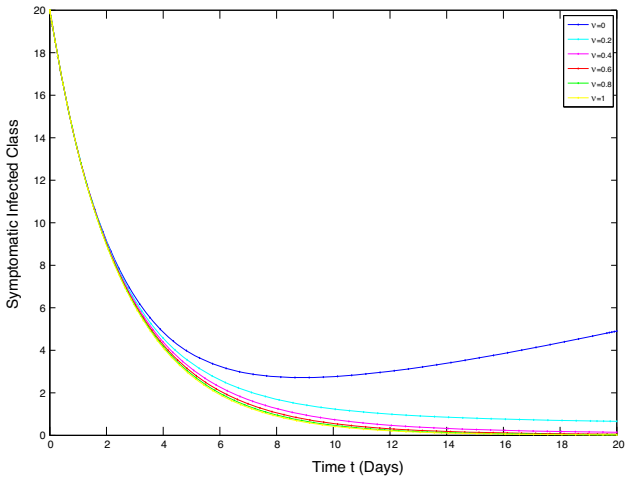

Fig. 20 Impact of v on symptomatic infected class

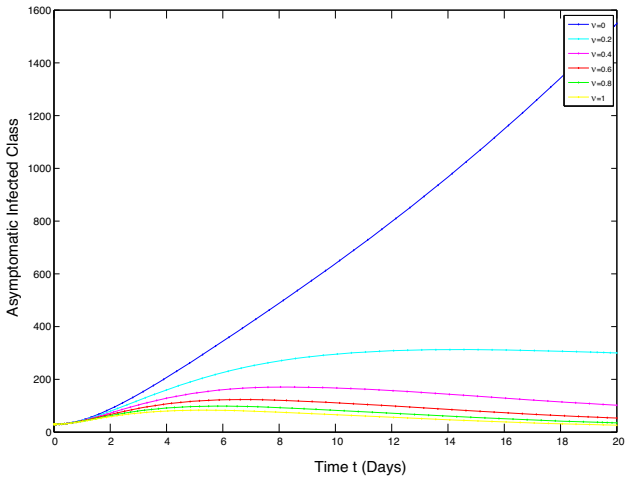

Fig. 21 Impact of v on asymptomatic infected class

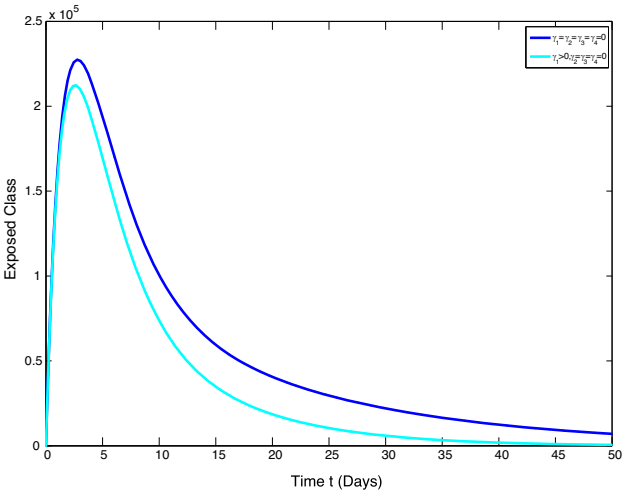

Fig. 23 Impact on Strategy I in exposed class

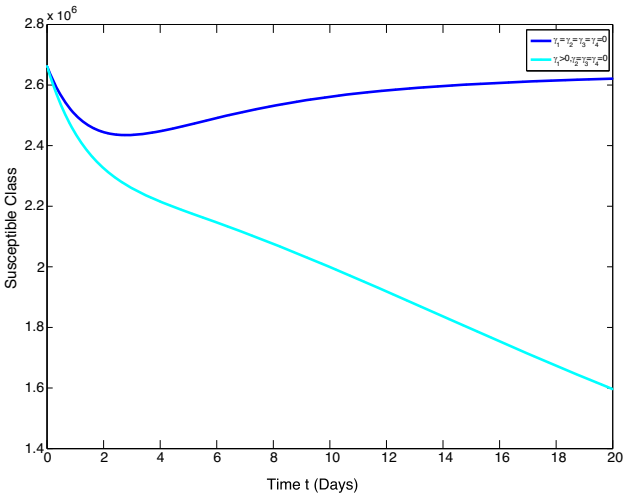

Fig. 22 Impact on Strategy I in susceptible class

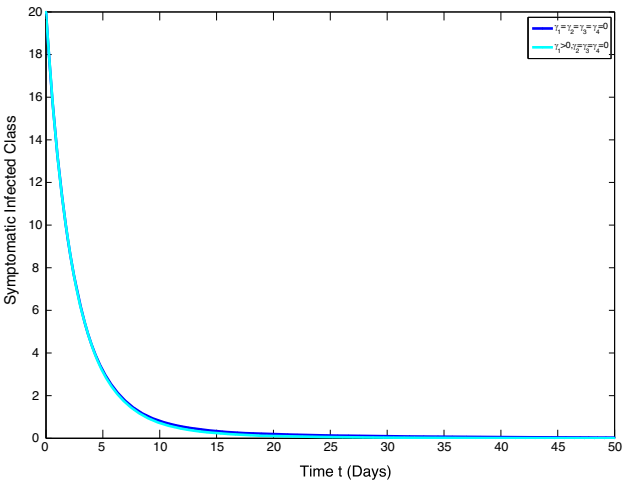

Fig. 24 Impact on Strategy I in symptomatic infected class

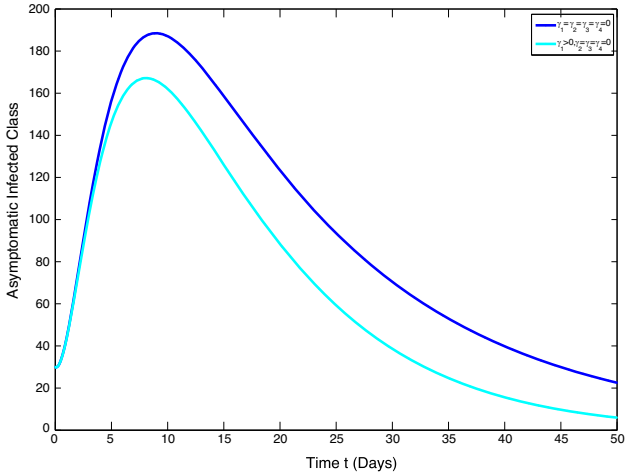

Fig. 25 Impact on Strategy I in asymptomatic infected class

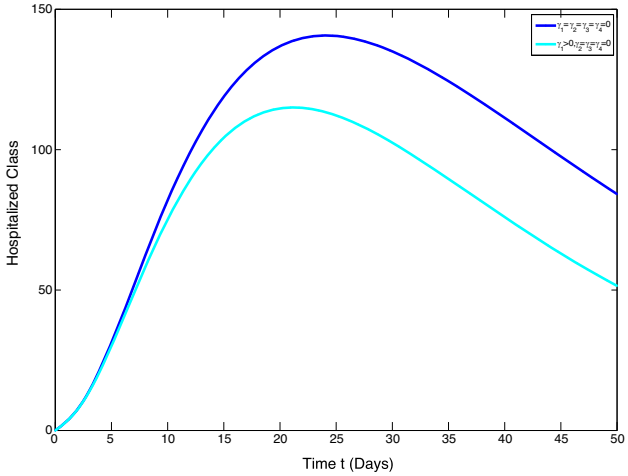

Fig. 26 Impact on Strategy I in hospitalized class

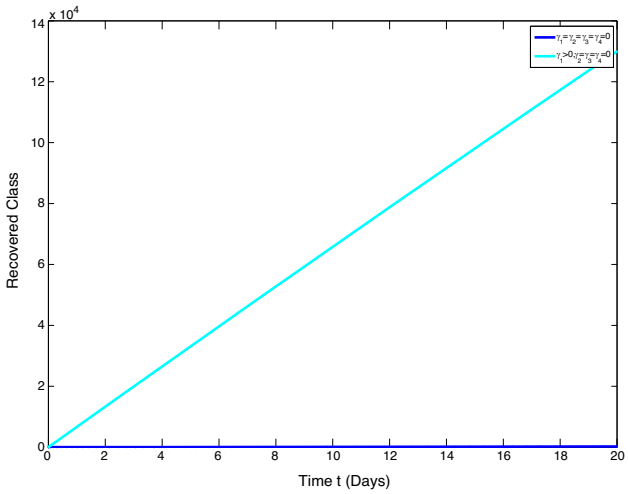

Fig. 27 Impact on Strategy I in recovered class

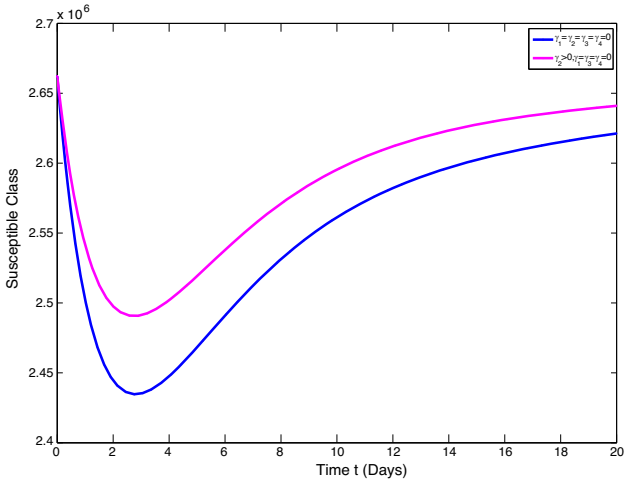

Fig. 28 Impact on Strategy II in susceptible class

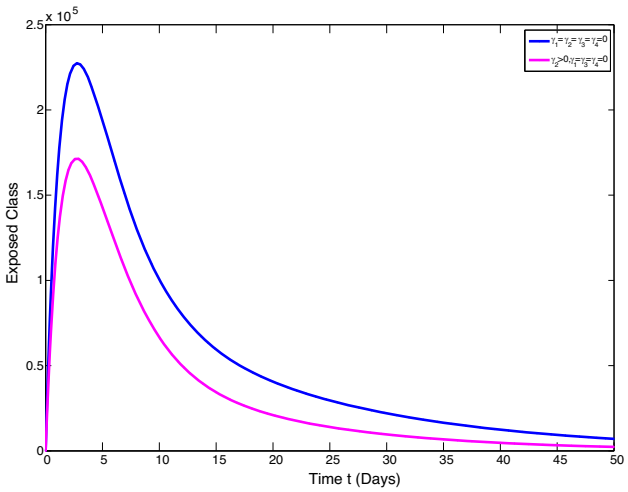

Fig. 29 Impact on Strategy II in exposed class

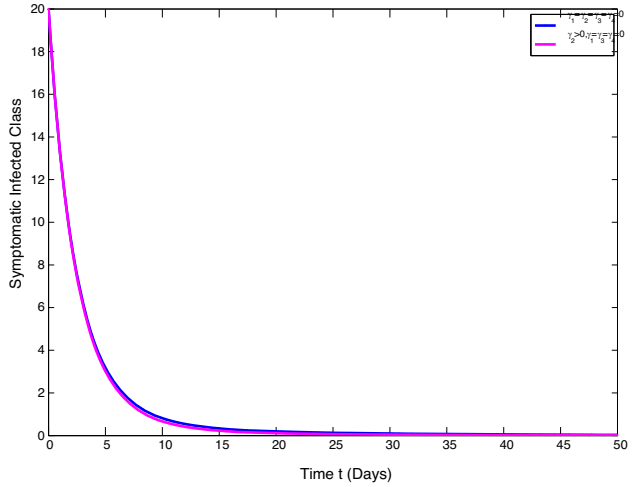

Fig. 30 Impact on Strategy II in symptomatic infected class

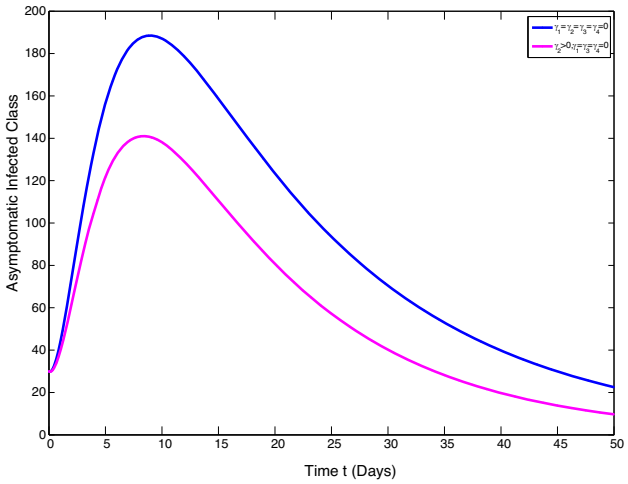

Fig. 31 Impact on Strategy II in asymptomatic infected class

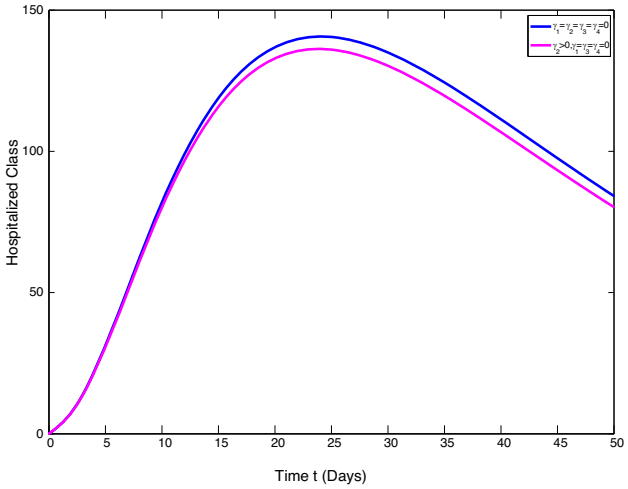

Fig. 32 Impact on Strategy II in hospitalized class

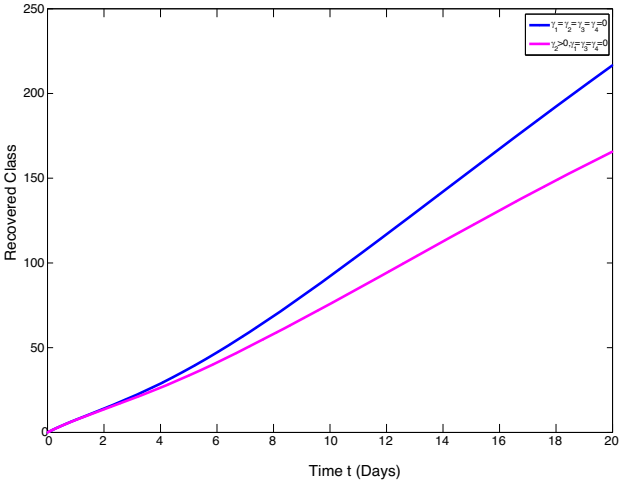

Fig. 33 Impact on Strategy II in recovered class

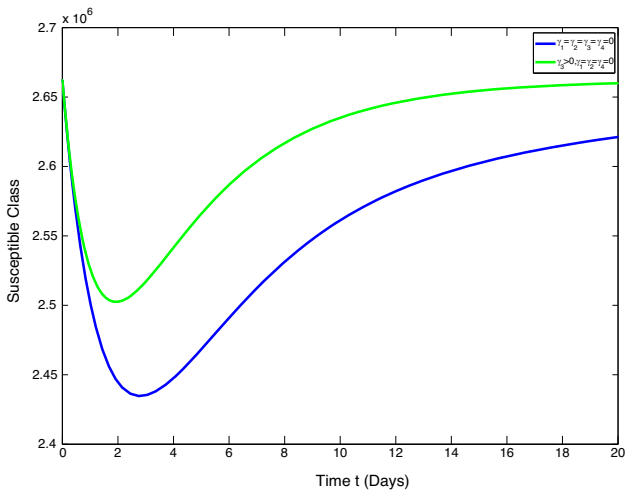

Fig. 34 Impact on Strategy III in susceptible class

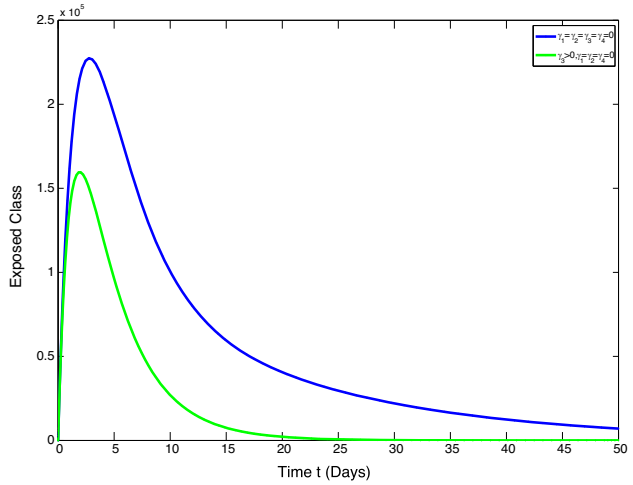

Fig. 35 Impact on Strategy III in exposed class

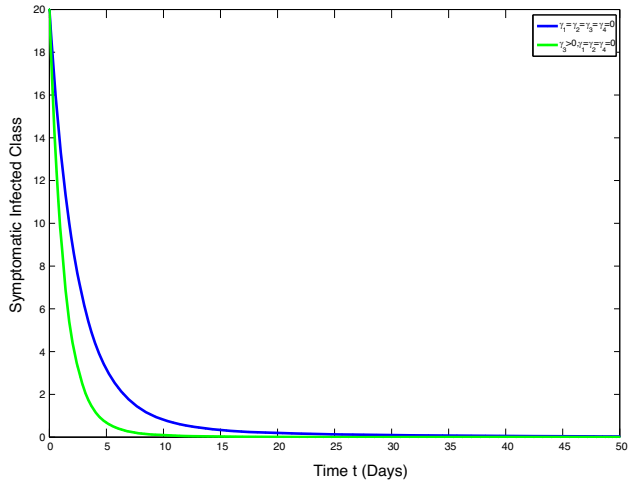

Fig. 36 Impact on Strategy III in symptomatic infected class

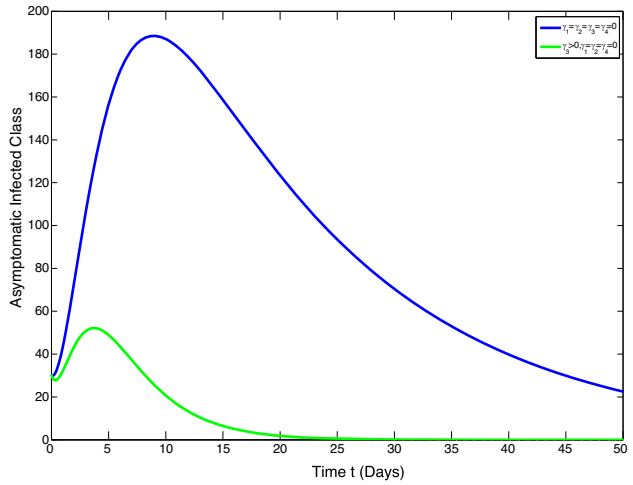

Fig. 37 Impact on Strategy III in asymptomatic infected class

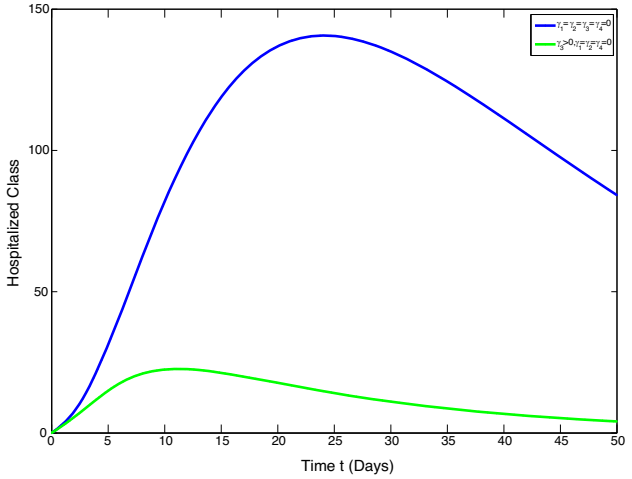

Fig. 38 Impact on Strategy III in hospitalized class

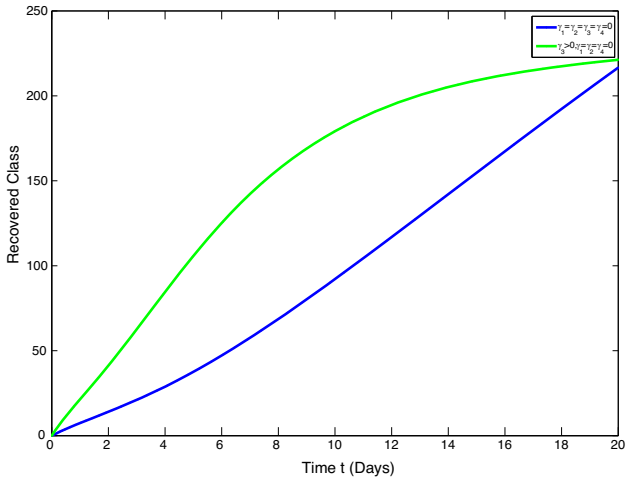

Fig. 39 Impact on Strategy III in recovered class

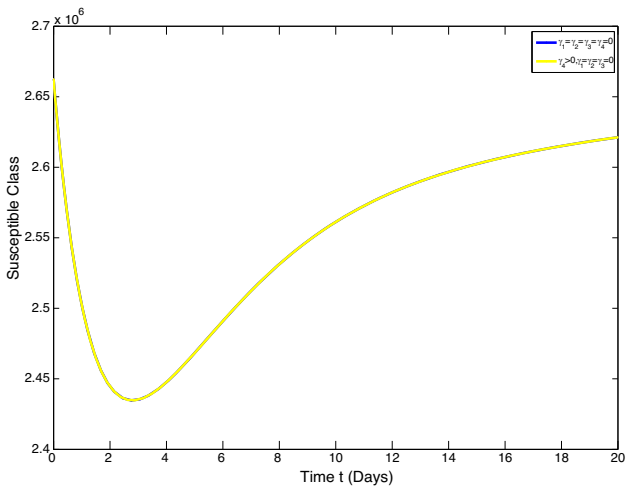

Fig. 40 Impact on Strategy IV in susceptible class

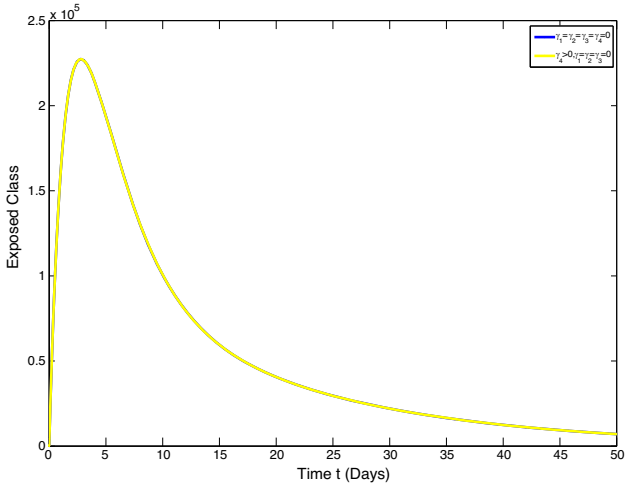

Fig. 41 Impact on Strategy IV in exposed class

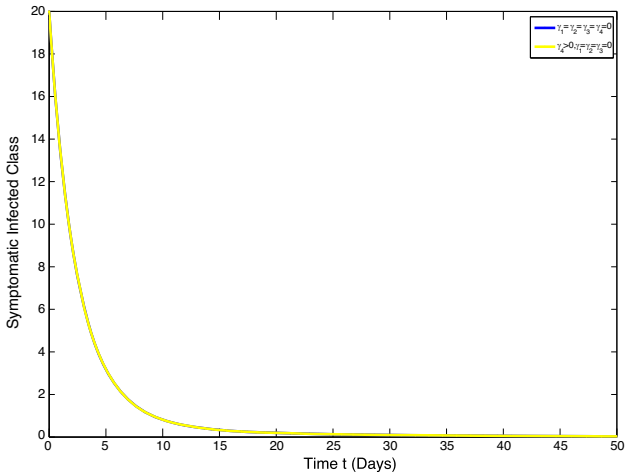

Fig. 42 Impact on Strategy IV in symptomatic infected class

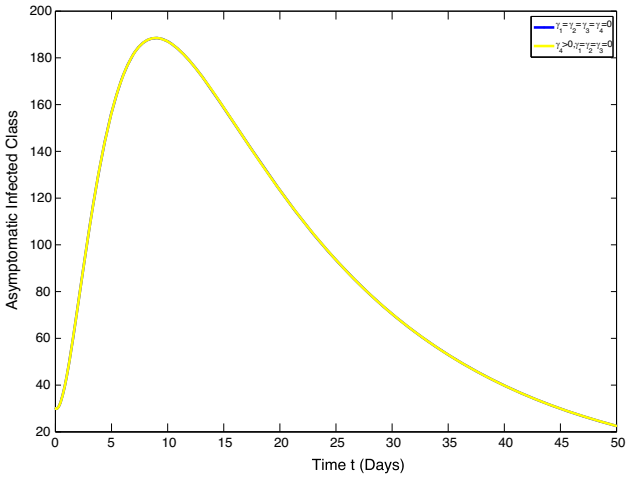

Fig. 43 Impact on Strategy IV in asymptomatic infected class

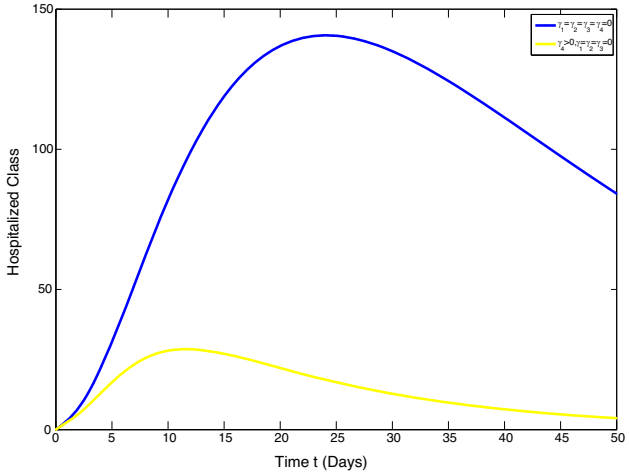

Fig. 44 Impact on Strategy IV in hospitalized class

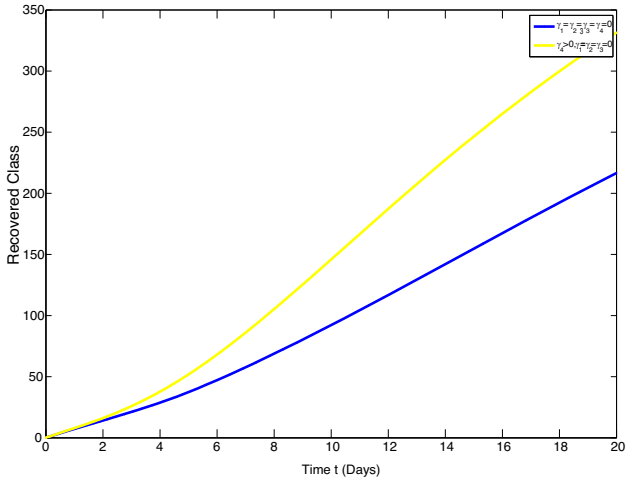

Fig. 45 Impact on Strategy IV in recovered class

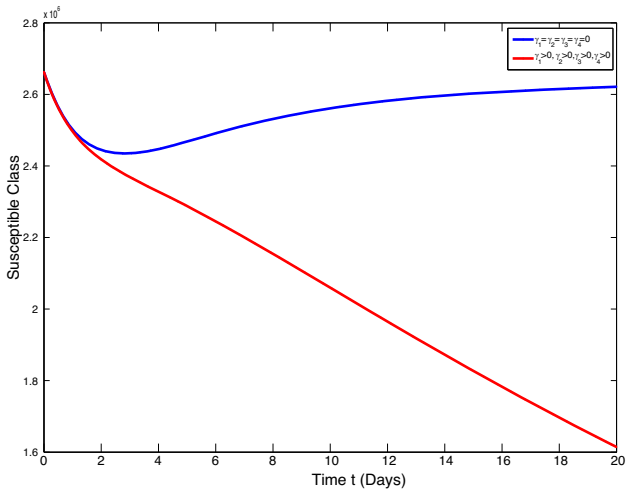

Fig. 46 Impact on Strategy V in susceptible class

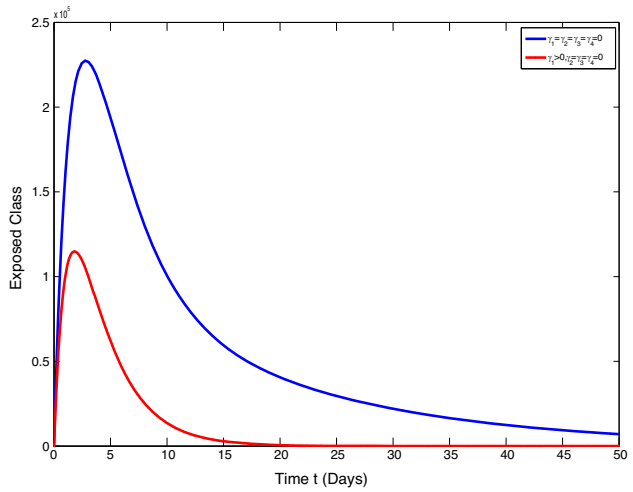

Fig. 47 Impact on Strategy V in exposed class

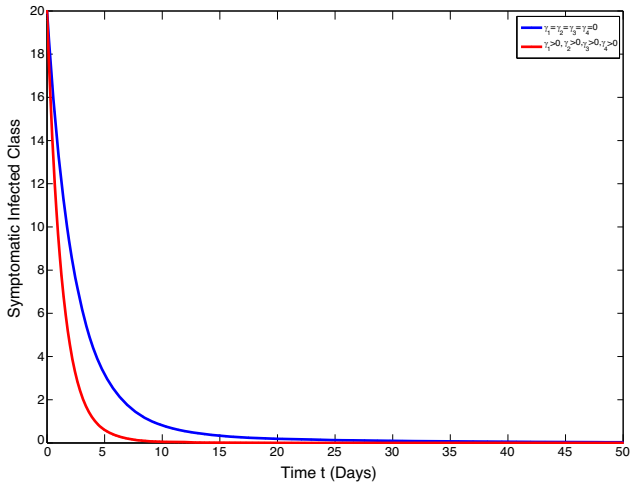

Fig. 48 Impact on Strategy V in symptomatic infected class

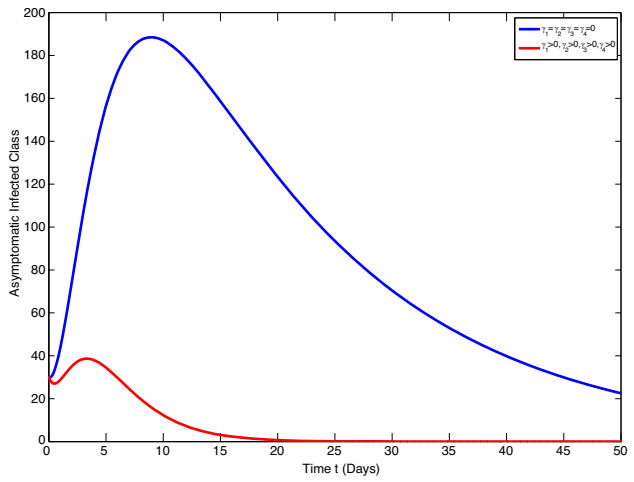

Fig. 49 Impact on Strategy V in asymptomatic infected class

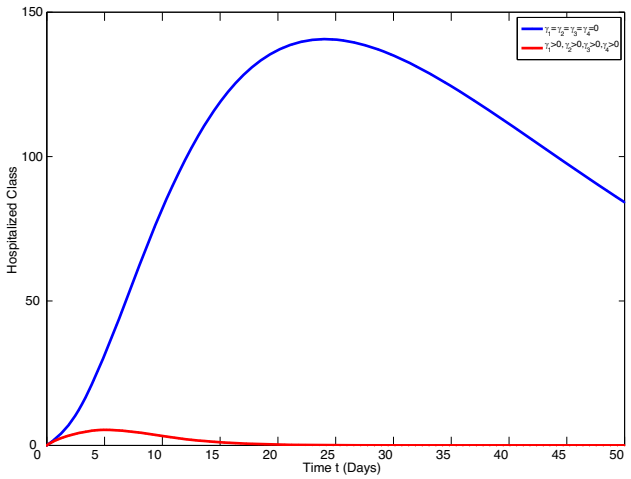

Fig. 50 Impact on Strategy V in hospitalized class

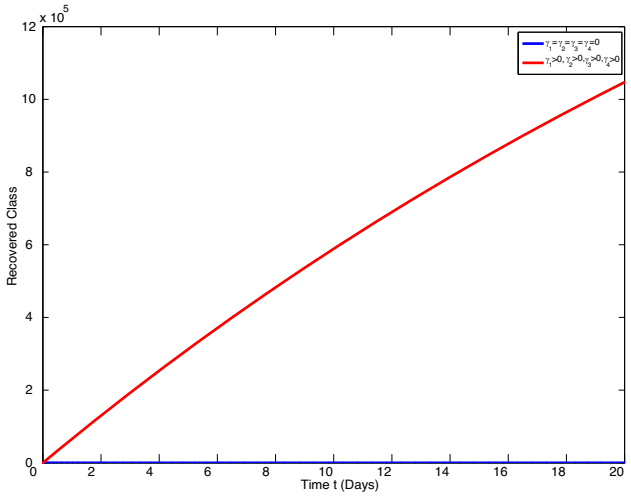

Fig. 51 Impact on Strategy V in recovered class

$$
\begin{aligned}
T_S(t_{f+1}) =& T_S(t_f) + \Psi(T_S(t_f), T_E(t_f), T_I(t_f), \\
& T_A(t_f), T_H(t_f), T_R(t_f)) \frac{t^a}{\Gamma(a+1)} \\
T_E(t_{f+1}) =& T_E(t_f) + \Psi(T_S(t_f), T_E(t_f), T_I(t_f), \\
& T_A(t_f), T_H(t_f), T_R(t_f)) \frac{t^a}{\Gamma(a+1)} \\
T_I(t_{f+1}) =& T_I(t_f) + \Psi(T_S(t_f), T_E(t_f), T_I(t_f), \\
& T_A(t_f), T_H(t_f), T_R(t_f)) \frac{t^a}{\Gamma(a+1)} \\
T_A(t_{f+1}) =& T_A(t_f) + \Psi(T_S(t_f), T_E(t_f), T_I(t_f), \\
& T_A(t_f), T_H(t_f), T_R(t_f)) \frac{t^a}{\Gamma(a+1)} \\
T_H(t_{f+1}) =& T_H(t_f) + \Psi(T_S(t_f), T_E(t_f), T_I(t_f), \\
& T_A(t_f), T_H(t_f), T_R(t_f)) \frac{t^a}{\Gamma(a+1)} \\
T_R(t_{f+1}) =& T_R(t_f) + \Psi(T_S(t_f), T_E(t_f), T_I(t_f), \\
& T_A(t_f), T_H(t_f), T_R(t_f)) \frac{t^a}{\Gamma(a+1)}
\end{aligned} \tag{17}
$$

where $f = 0, 1, \ldots, m-1$

Numerical interpretation and analysis

The following diagram shows the numerical results for the model in discussion. To achieve this, we employ the numerical simulation scheme we have chosen. Let us give some proper values to the parameters in the model they are: $A = 100, \pi = 0.0045,\ \sigma = 0.0001923,\ \eta = 0.0080, \psi_2 = 0.0414, \vartheta = 0.000037563, \vartheta_2 = 0.0037563, \xi_2 = 0.0714, \xi_1 = 0.05,\ \vartheta_1 = 0.0042310,\ \psi_1 = 0.36, \psi_3 = 0.05, \nu = 0.3563, \kappa = 0.0065$ and the initial conditions are $T_S(0) = 2662194, T_E(0) = 50, T_I(0) = 20, T_A(0) = 30, T_H(0) = 0, T_R(0) = 0$. Since this study does not focus on a specific disease, the parameter values are chosen based on reasonable assumptions to demonstrate the flexibility of the model. These assumed values allow us to analyze the model's behavior under different conditions. The model is designed to be adaptable, enabling researchers to adjust parameters according to real-world data for specific diseases in future studies.

Figures 4, 5, 6, 7, 8 and 9, show graphical representations for various values of a. In Figs. 4, 5, 6, 7, 8 and 9, we use Matlab to create an algorithm to simulate the findings. As α decreases, the system exhibits stronger memory effects, leading to slower transitions between compartments, which prolongs infection and recovery times. Conversely, higher α results in a behavior closer to integer-order models, where transitions occur more rapidly, leading to faster infection spread and recovery rates. These results emphasize how fractional-order derivatives capture realistic delays and memory effects in disease dynamics, making them a valuable tool for infectious disease modeling.

Interpretation of Contour Plots

Fig. 10, 11, 12, 13, 14, 15, 16 and Fig. 17 shows a contour plot depicting the dynamics of $\mathcal{R}_0$ in terms of $\nu, \eta, \sigma, \pi, \psi_1$ and ψ_2. Figures 10, 11, 12, 13 indicate how these variables affect the recovery rate of symptomatic infected people whereas 14 - Fig. 17 show the link between the rate of recovery of asymptomatic infected people and ν, η, σ, π in $\mathcal{R}_0$.

Impact of Precaution and natural Immunity

In this concept, precaution and natural immunity play a significant role. We may also boost our immunity by changing our diet behaviors and doing some yoga. So, as illustrated in Figs. 18, 19, 20 and 21, we are determining the efficacy of ν in susceptible, exposed, symptomatic, and asymptomatic infected classes. In order to reduce the complexity we fix $a = 1$.

Optimal control strategies

We define four separate control functions in our model. We may create five possible techniques to reduce the infection using these four controls, which are discussed below.

Strategy I:	$\gamma_1 > 0,\ \gamma_2 = \gamma_3 = \gamma_4 = 0$: Implementing γ_1 and not implementing $\gamma_2, \gamma_3, \gamma_4$.
Strategy II:	$\gamma_2 > 0,\ \gamma_1 = \gamma_3 = \gamma_4 = 0$: Implementing γ_2 and not implementing $\gamma_1, \gamma_3, \gamma_4$.
Strategy III:	$\gamma_3 > 0,\ \gamma_1 = \gamma_2 = \gamma_4 = 0$: Implementing γ_3 and not implementing $\gamma_1, \gamma_2, \gamma_4$.
Strategy IV:	$\gamma_4 > 0,\ \gamma_1 = \gamma_2 = \gamma_3 = 0$: Implementing γ_4 and not implementing $\gamma_1, \gamma_2, \gamma_3$.
Strategy V:	$\gamma_1 > 0, \gamma_2 > 0, \gamma_3 > 0, \gamma_4 > 0$: Implementing all control.

- *Strategy I*: $\gamma_1 > 0,\ \gamma_2 = \gamma_3 = \gamma_4 = 0$: Figs. 22, 23, 24, 25, 26 and 27 shows the impact of γ_1 in each compartment. γ_1 consists of measures taken to prevent those in the community who are uninfected yet susceptible to the epidemic. These may include measures such as spreading awareness to the public about the disease on how the disease is spread from person to person, practices individuals have to follow to prevent themselves from getting infected and continuous monitoring of the susceptible class to identify symptoms of

infection through tools such as health checkups and lab tests.

- *Strategy II*: $\gamma_2 > 0,\ \gamma_1 = \gamma_3 = \gamma_4 = 0$: Figs. 28, 29, 30, 31, 32 and 33 depicts the impact of γ_2 in each compartment. γ_2 are the strategies adopted towards those of the susceptible class who have been exposed to the infection, to prevent further outbreak if they are infected. This includes affirming through scientific methods that the person is indeed infected after getting exposed, suggesting practices to prevent further spread from them such as self or institutional quarantines if the disease is contagious or providing them with safe environments where these individuals won't come in contact with the disease any more.

- *Strategy III*: $\gamma_3 > 0,\ \gamma_1 = \gamma_2 = \gamma_4 = 0$: Figs. 34, 35, 36, 37, 38 and 39 illustrates the impact of γ_3 in each compartment. γ_3 are measures adopted towards infected persons to prevent them from further spreading the epidemic and also aiding them in getting cured. These measures implies to those who are infected but are asymptomatic or show mild symptoms which doesn't require specialised treatment at the moment. Control measures such as contact tracing to identify those who got exposed to their infection, continuous monitoring to know if infected individuals are showing symptoms or that their symptoms are getting worse are adopted.

- *Strategy IV*: $\gamma_4 > 0,\ \gamma_1 = \gamma_2 = \gamma_3 = 0$: Fig. 40, 41, 42, 43, 44 and 45 shows the impact of γ_4 in each compartment. γ_4 are measures applied to those who are infected but require hospital care specialised treatment. The aim of this strategy is to do what's required to bring the disease under control and get them cured with the help of hospital treatment.

- *Strategy V*: $\gamma_1 > 0,\ \gamma_2 > 0\ \gamma_3 > 0\ \gamma_4 > 0$: Figs. 46, 47, 48, 49, 50 and 51 shows the impact of combination of all the controls together in each compartment.

Carefully observing the graphs, we understood that strategy V has the highest impact in all the classes. Strategies I and II do not have much impact in symptomatic classes whereas strategy III has a novel impact in symptomatic class. Strategy IV has greater impact in hospitalized and recovery classes. From these, it is understood that each control has a vital role in all compartments. So we used all the four controls in strategy V inorder to have the benefits of all the four controls. Therefore, strategy V has positive impact in all compartments contributing reduction in infection class and hence establishes higher recovery rate.

Conclusion and future directions

In this study, we developed and analyzed a fractional-order mathematical model to enhance our understanding of infectious disease dynamics. By incorporating Caputo fractional-order derivatives (CFODs), the model offers a more accurate depiction of disease transmission, accounting for memory effects and long-term dependencies often neglected by traditional integer-order models. Through nonlinear analysis, we established the feasibility and boundedness of the solutions and computed the basic reproductive number ($\mathcal{R}_0$) to evaluate disease persistence. The existence and uniqueness of solutions were demonstrated using fixed-point theory, ensuring the model's mathematical robustness. To validate our theoretical findings, we applied the strong Euler numerical method to approximate solutions and used Matlab-based simulations to visualize disease dynamics. A sensitivity analysis was conducted to assess the importance of the key parameters identified in $\mathcal{R}_0$. Observing the results, we found that Strategy V had the most significant impact across all classes. Strategies I and II showed minimal effects on the symptomatic classes, whereas Strategy III exhibited a notable influence on the symptomatic group. Strategy IV had a substantial impact on the hospitalized and recovery classes. These findings indicate that each control strategy plays a crucial role across different compartments. Consequently, we combined all four controls into Strategy V, leveraging the advantages of each, which led to a positive impact across all compartments. This comprehensive approach contributed to a reduction in the infected class and an increase in the recovery rate, thus optimizing the overall disease control strategy.

Future research will focus on extending this model by incorporating real-world epidemiological data to validate its predictive capabilities and improve its applicability to specific infectious diseases. Additionally, we aim to conduct a bifurcation analysis to explore how changes in key parameters influence the transition between disease-free and endemic states. Another important direction is the integration of optimal control strategies to design effective intervention measures for disease mitigation. Furthermore, comparing the fractional-order model with classical integer-order models will help highlight the advantages of fractional derivatives in capturing realistic disease dynamics. Lastly, we plan to investigate generalized fractional operators, such as the Caputo-Fabrizio and Atangana-Baleanu derivatives, to assess their impact on

infectious disease modeling. These extensions will enhance the model's theoretical foundation and provide practical insights for epidemic control and public health decision-making.

Acknowledgements This article has been written with joint partial financial support from Phuket Rajabhat University, Thailand, and the RUSA Phase II 2.0 Grant No. F 24-51/2014-U.

Author Contributions S. A.J: Conceptualization, Methodology, Software, Validation, Formal analysis, Investigation, Resources, Data Curation, Writing - Original Draft, Writing - Review & Editing, Visualization. R. R: Methodology, Software, Validation, Formal analysis, Investigation, Supervision, Project administration, Writing - Original Draft, Writing - Review & Editing, Visualization. J.A: Software, Validation, Resources, Data Curation, Writing - Review & Editing, Visualization, Writing - Review & Editing. J. C: Methodology, Software, Validation, Resources, Data Curation, Writing - Original Draft, Writing - Review & Editing, Visualization. R.P.A: Software, Validation, Resources, Data Curation, Writing - Review & Editing, Visualization, Funding acquisition.

Data availability statement No datasets were generated or analysed during the current study.

Declarations

Conflict of interest The authors declare no Conflict of interest.

References

Agusto FB, Khan MA (2018) Optimal control strategies for dengue transmission in Pakistan. Math Biosci 305:102–121

Ahmed EM, El-Saka HA (2017) On a fractional order study of middle east respiratory syndrome corona virus (MERS-CoV). J Fract Calc Appl 8(1):118–126

Area I, NdaIrou F, Nieto JJ, Silva CJ, Torres DFM (2018) Ebola model and optimal control with vaccination constraints. J Ind Manag Optim 14(2):427–446

Baba BA, Bilgehan B (2021) Optimal control of a fractional order model for the COVID-19 pandemic. Chaos Solitons Fractals 144:110678

Ball F, Becker NG (2006) Control of transmission with two types of infection. Math Biosci 200(2):170–187

Brandeau ML, Zeric GS, Richter A (2003) Resource allocation for control of infectious diseases in multiple independent populations: beyond cost-effectiveness analysis. J Health Econ 22(4):575–598

Carvalho AR, Pinto CM, Baleanu D (2018) HIV/HCV coinfection model: a fractional-order perspective for the effect of the HIV viral load. Adv Differ Equ 2018(1):1–22

Castilho C (2006) Optimal control of an epidemic through educational campaigns. Electron J Differ Equ 2006(125):11

Chen BS, Li CW (2017) Big Tumorigenesis Mechanisms in Systems Cancer Biology via Big Database Mining and Network Modeling. In: Chen B-S, Li C-W (eds) Big mechanisms in systems biology. Academic Press, Cambridge, pp 431–526

Chitnis N, Hyman JM, Cushing JM (2008) Determining important parameters in the spread of malaria through the sensitivity analysis of a mathematical model. Bull Math Biol 70(5):1272–1296

Driessche PVD, Watmough J (2002) Reproduction numbers and subthreshold endemic equilibria for compartmental models of disease transmission. Math Biosci 180:29–48

El-Sayed AMA (2010) On the existence and stability of positive solution for a nonlinear fractional-order differential equation and some applications, Alexandria. J Math 1:1–10

Fantaye AK (2022) Modelling and stability analysis of cotton leaf curl virus (CLCuV) transmission dynamics in cotton plant. J Appl Math 12

Fantaye AK (2024) Fractional order for the transmission dynamics of coffee berry diseases (CBD). Eur J Appl Math. 1–18. https://doi.org/10.1017/S0956792524000780

Fantaye AK, Birhanu ZK (2023) Modeling and analysis for the transmission dynamics of cotton leaf curl virus using fractional order derivatives. Heliyon 9:e16877

Fantaye AK, Goshu MD, Zeleke BB, Gessesse AA, Endalew MF, Birhanu ZK (2022) Mathematical model and stability analysis on the transmission dynamics of skin sores. Epidemiol Infect 150:e207. https://doi.org/10.1017/S0950268822001807

Herdicho FF, Jose SA, Jirawattanapanit A, Park T (2025) Fractional derivative models in COVID-19 dynamics: application to symptom severity and hospital resource allocation in South Korea. J Appl Math Comput. https://doi.org/10.1007/s12190-024-02359-y

Hethcote HW (2000) The mathematics of infectious diseases. SIAM Rev 42(4):599–653

Jose SA, Raja R, Omede BI, Agarwal RP, Alzabut J, Cao J, Balas VE (2022) Mathematical modeling on co-infection: transmission dynamics of zika virus and dengue fever. Nonlinear Dyn. https://doi.org/10.1007/s11071-022-07581-6

Jose SA, Raja R, Dianavinnarasi J, Baleanu D, Jirawattanapanit A (2023) Mathematical modeling of chickenpox in Phuket: efficacy of precautionarym measures and bifurcation analysis. Biomed Signal Process Control 84:104714

Jose SA, Yaagoub Z, Joseph D, Ramachandran R, Jirawattanapanit A (2024) Computational dynamics of a fractional order model of chickenpox spread in Phuket province. Biomed Signal Process Control 91:105994

Khaminsou B, Thaiprayoon C, Sudsutad W, Aby JS (2021) Qualitative analysis of a proportional Caputo fractional Pantograph differential equation with mixed nonlocal conditions. Nonlinear Funct Anal Appl 26(1):197–223

Khan MA, Ullah S, Kumar S (2021) A robust study on 2019-nCOV outbreaks through non-singular derivative. Eur Phys J Plus 136:168

Kim Y, Lee S, Chu C, Choe S, Hong S, Shin Y (2016) The characteristics of middle eastern respiratory syndrome coronavirus transmission dynamics in South Korea. Osong Public Health and Res Perspect 7(1):49–55

Lee D, Masud MA, Kim BN, Oh C (2017) Optimal control analysis for the MERS-CoV outbreak: South Korea perspectives. J Korean Soc Ind Appl Math 21(3):143–154

Lin W (2007) Global existence theory and chaos control of fractional differential equations. J Math Anal Appl 332:709–726

McNabb A (1986) Comparison theorems for differential equations. J Math Anal Appl 119:417–428

Nelson SP, Raja R, Eswaran P et al (2024) Modeling the dynamics of Covid-19 in Japan: employing data-driven deep learning approach. Int J Mach Learn Cyber. https://doi.org/10.1007/s13042-024-02301-5

Panigoro HS, Rahmi E, Bonyah E, Akgul A, Misro MY, Jose SA (2025) The impact of competitions on the dynamics of a two predators—one prey model involving caputo fractional-order derivative. Fractals. https://doi.org/10.1142/S0218348X25400778

Pinto Carla MA, Carvalho Ana RM (2017) A latency fractional order model for HIV dynamics. J Comput Appl Math 312(C):240–256
Podlubny I (1998) Fractional differential equations: an introduction to fractional derivatives, fractional differential equations, to methods of their solution and some of their applications. Elsevier
Shamil E, Jose SA, Panigoro HS, Jirawattanapanit A, Omede BI, Yaagoub Z (2014) Understanding COVID-19 propagation: a comprehensive mathematical model with caputo fractional derivatives for Thailand. Front Appl Math Stat 10:1374721
Shen ZH, Chu YM, Khan MA, Muhammad S, Al-Hartomy OA, Higazy M (2021) Mathematical modeling and optimal control of the COVID-19 dynamics. Results Phys 31(2021):105028
Silva CJ, Torres DFM (2018) Modeling and optimal control of HIV/AIDS prevention through prep. Discrete Contin Dyn Syst 11(1):119–141
Silva CJ, Maurer H, Torres DFM (2017) Optimal control of a tuberculosis model with state and control delays. Math Biosci Eng 14(1):321–337
Sweilam NH, AL-Mekhlafi SM, Mohammed ZN, Baleanu D (2020) Optimal control for variable order fractional HIV/AIDS and malaria mathematical models with multi-time delay. Alex Eng J 59(5):3149–3162
Tahir M, Ali Shah SI, Zaman G, Khan T (2019) Stability behaviour of mathematical model MERS Corona virus spread in population. Filomat 33(12):3947–3960
Tamilalagan P, Karthiga S, Manivannan P (2021) Dynamics of fractional order HIV infection model with antibody and cytotoxic t-lymphocyte immune responses. J Comput Appl Math 382(2):113064
Teklu SW (2024a) Insight into the optimal control strategies on corruption dynamics using fractional order derivatives. Sci Afr 23:e02069
Teklu SW (2024b) Impacts of optimal control strategies on the HBV and COVID-19 co-epidemic spreading dynamics. Sci Rep 14:5328
Teklu SW, Yohannes FA (2024) Analysis of the hate speech and racism co-existence dissemination model with optimal control strategies. Chaos Solitons Fractals X 12:100109
Teklu SW, Meshesha AA, Ullah S (2024) Analysis of optimal control strategies on the fungal *Tinea capitis* infection fractional order model with cost-effective analysis. Sci Rep 14:1508
Thomas R, Jose SA, Raja R, Alzabut J, Cao J, Balas Valentina E, Niezabitowski M (2022) Modeling and analysis of SEIRS epidemic models using homotopy perturbation method: a special outlook to 2019-nCoV in India. Int J Biomath. https://doi.org/10.1142/S1793524522500590
Van-Driessche D, Watmough J (2002) Reproduction numbers and subthreshold endemic equilibria for compartmental models of disease transmission. Math Biosci 180(1):29–48
Vargas-De-Léon C (2015) Volterra-type Lyapunov functions for fractional-order epidemic systems. Commun Nonlinear Sci Numer Simul 24(1–3):75–85
Wang CG, Chen BS (2022) Multiple-molecule drug repositioning for disrupting progression of SARS-CoV-2 infection by utilizing the systems biology method through host-pathogen-interactive time profile data and DNN-based DTI model with drug design specifications. Stresses 2:405–436
Zafar ZUA, Rehan K, Mushtaq M (2017) HIV/AIDS epidemic fractional-order model. J Differ Equ Appl 23(7):1298–1315